Major perturbations in the global carbon cycle and photosymbiont-bearing planktic foraminifera during the early Eocene

Valeria Luciani[1], Gerald R. Dickens[2,3], Jan Backman [2], Eliana Fornaciari[4], Luca Giusberti[4], Claudia Agnini[4], Roberta D'Onofrio[1]

[1]Department of Physics and Earth Sciences, Ferrara University, Polo Scientifico Tecnologico, via G. Saragat 1, 44100, Ferrara, Italy

[2]Department of Geological Sciences, Stockholm University, SE-10691 Stockholm, Sweden

[3]Department of Earth Science, Rice University, Houston, TX 77005, USA

[4]Department of Geosciences, Padova University, via G. Gradenigo 6, 35131, Padova, Italy

Correspondence to: V. Luciani (valeria.luciani@unife.it)

Abstract. A marked switch in the abundance of the planktic foraminiferal genera *Morozovella* and *Acarinina* occurred near the start of the Early Eocene Climatic Optimum (EECO), a multi-million-year interval when Earth surface temperatures reached their Cenozoic maximum. Stable carbon and oxygen isotope data of bulk sediment are presented from across the EECO at two locations: Possagno in northeast Italy, and DSDP Site 577 in the northwest Pacific. Relative abundances of planktic foraminifera are presented from these two locations, as well as from ODP Site 1051 in the northwest Atlantic. All three sections have good stratigraphic markers, and the $\delta^{13}C$ records at each section can be correlated amongst each other and to $\delta^{13}C$ records at other locations across the globe. These records show that a series of negative carbon isotope excursions (CIEs) occurred before, during and across the EECO, which is defined here as the interval between the "J" event and the base of *Discoaster sublodoensis*. Significant though ephemeral modifications in planktic foraminiferal assemblages coincide with some of the short-term CIEs, which were marked by increases in the relative abundance of acarininids, similar to what happened across established hyperthermal events in Tethyan settings prior to the EECO. Most crucially, a temporal link exists between the onset of the EECO, carbon cycle changes during this time, and the demise of morozovellids. Possible causes are multiple, and may include temperature effects on photosymbiont-bearing planktic foraminifera and changes in ocean chemistry.

1 Introduction

Cenozoic Earth surface temperatures attained their warmest state during the Early Eocene Climatic Optimum (EECO). This was a 2-4 Myr long interval (discussed below) centered at ca. 51 Ma (**Figure 1**), when average high latitude temperatures exceeded those at present-day by at least 10°C (Zachos et al., 2008; Huber and Caballero, 2011; Hollis et al., 2012; Pross et al., 2012; Inglis et al., 2015). Several short-term (<200 kyr) global warming events (**Figure 1**) occurred before the EECO. The Paleocene Eocene Thermal Maximum (PETM) provides archetypical example: about 55.9 Ma (Vandenberghe et al., 2012; Hilgen et al., 2015) temperatures soared an additional 5-6°C relative to background conditions (Sluijs et al., 2006, 2007; Dunkley Jones et al., 2013). Evidence exists for at least two other significant warming events (Cramer et al., 2003; Lourens et al., 2005; Röhl et al., 2005; Thomas et al., 2006; Nicolo et al., 2007; Agnini et al., 2009; Coccioni et al., 2012; Lauretano et al., 2015; Westerhold et al., 2015): one ca. 54.1 Ma and named H-1 or Eocene Thermal Maximum 2 (ETM-2, also referred as ELMO), and one at 52.8 Ma and variously named K, X, or ETM-3 (hereafter called K/X). However, additional brief warming events may have spanned the early Eocene (above references; Kirtland-Turner et al., 2014), and the EECO may comprise a series of successive events (Slotnick et al., 2012). Both long-term and short-term intervals of warming corresponded to major changes in global carbon cycling, although the precise timing between these parameters remains insufficiently resolved.

In benthic foraminiferal stable isotope records for the early Paleogene (**Figure 1**), $\delta^{18}O$ serves as a proxy for deep-water temperature, while $\delta^{13}C$ relates to the composition of deep-water dissolved inorganic carbon (DIC). The highest $\delta^{13}C$ values of the Cenozoic occurred at ca. 58 Ma. From this Paleocene Carbon Isotope Maximum (PCIM), benthic foraminiferal $\delta^{13}C$ values plunge by approximately 2.5 ‰ to reach a near Cenozoic minimum at or near the

start of the EECO, and subsequently rise by approximately 1.5 ‰ across this interval (Zachos et al., 2001, 2008; Cramer et al., 2009). Benthic foraminiferal $\delta^{13}C$ records also exhibit prominent negative carbon isotope excursions (CIEs) across the three hyperthermals mentioned above (Kennett and Stott, 1991; Littler et al., 2014; Lauretano et al., 2015). Crucially, at least from the late Paleocene to the start of the EECO, similar $\delta^{13}C$ records occur in other carbon-bearing phases, such as bulk marine carbonate, planktic foraminifera, and various marine and terrestrial organic carbon compounds (Shackleton, 1986; Lourens et al., 2005; Nicolo et al., 2007; Agnini et al., 2009, 2015; Leon-Rodriguez and Dickens, 2010; Abels et al., 2012; Coccioni et al., 2012; Sluijs and Dickens, 2012; Slotnick et al. 2012, 2015a; Clyde et al., 2013). This strongly suggests that observed changes in $\delta^{13}C$, both long-term trends as well as short-term perturbations, represent variations in the input and output of ^{13}C-depleted carbon to the exogenic carbon cycle (Shackleton, 1986; Dickens et al., 1995; Dickens, 2000; Kurtz et al., 2003; Komar et al., 2013).

Significant biotic changes occur in terrestrial and marine environments during times when the early Paleogene $\delta^{18}O$ and $\delta^{13}C$ records show major variations. This has been recognized for the PETM, where land sections exhibit a prominent mammal turnover (Gingerich 2001, 2003; McInerney and Wing, 2011; Clyde et al., 2013), and bathyal-abyssal marine sections reveal a profound benthic foraminiferal extinction (Thomas, 1998) as well as appearances of planktic excursion taxa (Kelly et al., 1996, 1998; Crouch et al., 2001). Major plant and mammal turnovers also occurred during the longer EECO (Wing et al., 1991; Zonneveld et al., 2000; Wilf et al., 2003; Falkowski et al., 2005; Woodbourne et al., 2009; Figueirido et al., 2012). In the marine realm, evolutionary trends across the EECO have been noted, in particular the inception of modern calcareous nannofossil community structure (Agnini et al., 2006; Schneider et al., 2011; Shamrock et al., 2012) and possibly the same for diatoms (Sims et al., 2006; Oreshkina, 2012). These observations, both from continents and

95 the oceans, support an overarching hypothesis that climate change drives biotic evolution.
96 Planktic foraminiferal assemblages are abundant in carbonate bearing marine sediments
97 and display distinct evolutionary trends that often can be correlated to climate variability
98 (Schmidt et al., 2004; Fraass et al., 2015). This is especially true in the early Paleogene, even
99 though the relationship between climate variability and planktic foraminiferal evolution
100 remains insufficiently known. At the beginning of the Eocene, planktic foraminifera had
101 evolved over ca. 10 Myr following the Cretaceous-Paleogene mass extinction event. Several
102 early Paleogene phylogenetic lines evolved, occupying different ecological niches in the
103 upper water column. Subsequently, a major diversification occurred during the early Eocene,
104 which resulted in a peak of planktic foraminiferal diversity during the middle Eocene (Norris,
105 1991; Schmidt et al., 2004; Pearson et al., 2006; Aze et al., 2011; Fraas et al., 2015).
106 In this study, we focus on the evolution of two planktic foraminiferal genera:
107 morozovellids and acarininids (**Figure 1**). These two genera belong to the "muricate group",
108 a term derived from the muricae that form conical pustules on the test wall. These two genera
109 are of particular interest because of their dominance among tropical and subtropical
110 assemblages of the early Paleogene oceans, and because these genera show a major turnover
111 in taxonomic diversity close to the beginning of the EECO, one that comprises and species
112 reduction among morzovellids and species diversification among acarininids (**Figure 1**) (Lu
113 and Keller, 1995; Lu et al., 1998; Pearson et al., 2006; Aze et al., 2011).
114 Numerous lower Eocene sedimentary sections from lower latitudes contain well-
115 preserved planktic foraminifera. These foraminiferal assemblages presumably reflect
116 relationships between climate and carbon cycling across the EECO. The present problem is
117 that no section examined to date provides counts of foraminiferal assemblages, detailed stable
118 isotope records and robust planktic foraminiferal biostratigraphies across the entire EECO.
119 Indeed, at present, only a few sites have detailed and interpretable stable isotope records

120 across much of the EECO (Slotnick et al., 2012, 2015a; Kirtland-Turner et al., 2014). As a
121 consequence, any relationship between climatic perturbations during the EECO and the
122 evolution of planktic foraminifera remains speculative. Here, we add new data from three
123 locations: the Possagno section from the western Tethys, DSDP Site 577 from the tropical
124 Pacific Ocean, and ODP Site 1051 from the subtropical Atlantic Ocean **(Figure 2**). These
125 sections hence represent a wide longitudinal span of low latitude locations during the early
126 Paleogene. By comparing stable isotope and planktic foraminiferal records at these three
127 locations, we provide a new foundation for understanding why the abundances of acarininids
128 and morozovellids changed during the EECO.
129
130 **2 The Early Eocene Climatic Optimum**
131
132 Evidence for extreme Earth surface warmth during a multi-million year time interval of the
133 early Eocene is overwhelming, and comes from many studies, utilizing both marine and
134 terrestrial sequences, and both fossil and geochemical proxies (Huber and Caballero, 2011;
135 Hollis et al., 2012; Pross et al., 2012). However, a definition for the EECO, including the
136 usage of "optimum", endures as a perplexing problem circa 2015. This is for several reasons,
137 including the basic facts that: (i) temperature should not define time increments, (ii) clearly
138 correlative records across the middle of the early Eocene with temporal resolution less than
139 50 kyr remain scarce, and (iii) absolute ages across the early Eocene have changed
140 significantly (Berggren et al., 1995; Vandenberghe et al., 2102). As a consequence, various
141 papers discussing the EECO give different ages and durations (e.g., Yapp, 2004; Lowenstein
142 and Demicco, 2006; Zachos et al., 2008; Woodburne et al., 2009; Smith et al., 2010; Hollis et
143 al., 2012; Slotnick et al., 2012; Puljalte et al., 2015).
144 The EECO, at least as presented in many papers, refers to the time of minimum $\delta^{18}O$

145 values in “stacked” benthic foraminifera stable isotope curves (**Figure 1**). These curves were
146 constructed by splicing together multiple $\delta^{18}O$ records generated at individual locations onto
147 a common age model. However, the stacked curves (Zachos et al., 2001, 2008; Cramer et al.,
148 2009) show significant variance in $\delta^{18}O$ across the middle of the early Eocene. Some of this
149 variance belies imprecisely calibrated records at individual sites, where cores do not align
150 properly in the depth domain (Dickens and Backman, 2013). Some of this variance probably
151 reflects a dynamic early Eocene climate regime, where average temperatures and atmospheric
152 pCO_2 across Earth changed significantly, perhaps on orbital time scales (Smith et al., 2010;
153 Slotnick et al., 2012, 2015a; Kirtland-Turner et al., 2014).
154 The onset of low benthic foraminiferal $\delta^{18}O$ values closely corresponds with a long-term
155 minimum in $\delta^{13}C$ values (**Figure 1**). This is important for stratigraphic reasons because the
156 two stable isotope curves were generated using the same benthic foraminiferal samples, but
157 $\delta^{13}C$ records at different locations should necessarily correlate in the time domain (unlike
158 $\delta^{18}O$ and temperature). The rationale for such carbon isotope stratigraphy lies in the rapid
159 cycling of carbon across Earth’s surface (Shackleton, 1986; Dickens, 2000).
160 The Eocene minimum in $\delta^{13}C$ corresponds to the K/X event (**Figure 1**), which happened
161 in polarity chron C24n.1n and approximately 3 Myr after the PETM (Agnini et al., 2009;
162 Leon-Rodriguez and Dickens, 2010; Slotnick et al., 2012; Dallanave et al., 2015; Lauretano
163 et al., 2015; Westerhold et al., 2015). However, in several detailed studies spanning the early
164 Eocene, changes in long-term trends appear to have occurred about 400 kyr before K/X, and
165 at an event called “J” (after Cramer et al., 2003), which happened near the boundary of
166 polarity chrons C24n.2r and C24n.3n (Slotnick et al., 2015a; Lauretano et al., 2015). Notably,
167 the long-term late Paleocene-early Eocene decrease in benthic foraminifera $\delta^{18}O$ records at
168 Site 1262 on Walvis Ridge ceases at the J event (Lauretano et al., 2015).
169 The end of the EECO has received limited attention from a stratigraphic perspective. In

sections from the Clarence River Valley, New Zealand, a major lithologic change from limestone to marl coincides with the J event (Slotnick et al., 2012, 2015a; Dallanave et al., 2015). The marl-rich unit, referred to as "Lower Marl", has been interpreted to reflect enhanced terrigenous supply to a continental margin because of greater temperature and enhanced seasonal precipitation. It has been suggested further that Lower Marl expresses the EECO (Slotnick et al., 2012; Dallanave et al., 2015). The top of Lower Marl, and a return to limestone deposition, lies within the upper part of polarity chron C22n (Dallanave et al., 2015). This is interesting because it approximates the time of general cooling at several locations with polarity chrons and proxy records of warming (Hollis et al., 2012; Pross et al., 2012). It is also useful because the end of the EECO thus lie close to a well documented and widespread calcareous nannofossil biohorizon, the base of *Discoaster sublodoensis*.

Without an accepted definition in the literature, we tentatively present the EECO as the duration of time between the J event and the base of *D. sublodoensis.* This interval thus begins at about 53 Ma and ends at about 49 Ma on the 2012 Time Scale (GTS; Vandenberghe et al., 2012). However, while the EECO was characterized by generally warm conditions, numerous fluctuations in average temperature likely occurred.

3 Sites and stratigraphy

3.1 Possagno, Venetian Prealps, Tethys

An Upper Cretaceous through Miocene succession crops out at the bottom of the Monte Grappa Massif in the Possagno area, about 60 km northwest of Venice. The lower to middle Eocene, the primary focus of this study, is represented by the Scaglia beds. These sedimentary rocks represent pelagic and hemipelagic sediment that accumulated at middle to

lower bathyal depths (Cita, 1975; Thomas, 1998) in the western part of the Belluno Basin, a Mesozoic–Cenozoic paleogeographic unit of the Southern Alps (Bosellini, 1989).

A quarry at 45°51.0' N and 11°51.6' E exposed a 66 m thick section of the Scaglia beds (**Figure 3**). This section was examined for its stratigraphy (Agnini et al., 2006; Luciani and Giusberti, 2014), and shown to extend from just below the PETM to within lower Chron C20r in the lower middle Eocene. Like other lower Paleogene sections of the Venetian Pre-alps (Giusberti et al., 2007), a Clay Marl Unit (CMU) with a prominent negative CIE marks the PETM.

The Possagno section appears to be continuous, but with an important decrease in sedimentation rate (up to ca. 1.4 m/Myr) between 14.66 m and 15.51 m within Chron C23r near the start of the EECO and predating the onset of a major increase in discoasters (Agnini et al., 2006).

3.2 Site 577, Shatsky Rise, Western Pacific

Deep Sea Drilling Project (DSDP) Leg 86 drilled Site 577 at 32°26.5' N, 157°43.4' E, and 2680 m water depth, on the Shatsky Rise, which is a large igneous plateau in the NW Pacific with a relatively thin veneer of sediment (Shipboard Scientific Party 1985). During the early Eocene, this site was located closer to 15° N (**Figure 2**), and probably at a slightly shallower water depth (Ito and Clift, 1998).

Two primary holes were drilled at Site 577. Both Hole 577* and Hole 577A recovered portions of a nominally 65 m thick section of Upper Cretaceous through lower Eocene nannofossil ooze. Similar to the Possagno section, the lower Paleogene interval has biomagnetostratigraphic information (Bleil, 1985; Monechi et al., 1985; Backman, 1986; Lu and Keller, 1995; Dickens and Backman, 2013). Stable isotope records of bulk carbonate

have been generated for sediment from Cores 577*9H and 577A-9H (Cramer et al. 2003).

The composition and relative abundances of planktic foraminifera were nicely documented at Site 577 (Lu, 1995; Lu and Keller, 1995), and show a marked turnover between morozovellids and acaraninids during the early Eocene. These data, however, have remained on an out-dated view for the stratigraphy at this location, where cores were not originally aligned to account for gaps and overlaps (Dickens and Backman, 2013). As will become obvious later, the main phase of the EECO spans Cores 577*-8H and 577A-8H.

3.3 Site 1051, Blake Nose, Western Atlantic

The Blake Nose is a gentle ramp extending from 1000 m to 2700 m water depth east of Florida (Norris et al, 1998). The feature is known for a relatively thick sequence of middle Cretaceous through middle Eocene sediment with minimal overburden. Ocean Drilling Program (ODP) Leg 171B drilled and cored this sequence at several locations, including Site 1051 at 30°03.2' N, 76°21.5' W, and 1994 m water depth (Shipboard Scientific Party 1998). The site was located slightly to the south during the early Eocene (**Figure 2**). Benthic foraminiferal assemblages indicate a lower bathyal depth (1000-2000 m) during the late Paleocene and middle Eocene (Norris et al., 1998), although Bohaty et al. (2009) estimated a paleodepth of about 2200 m for sedimentation ca. 50 Ma.

Sediments from 452.24 to 353.10 meters below sea floor (mbsf) at Site 1051 consist of lower to middle Eocene carbonate ooze and chalk (Shipboard Scientific Party, 1998). Although the site comprises two holes (1051A and 1051B), with core gaps and core overlaps existing at both (Shipboard Scientific Party, 1998), the impact of these depth offsets upon age is less than at Site 577, because of higher overall sedimentation rates.

The Eocene section at Site 1051 has good sediment recovery, except an interval between 382 mbsf and 390 mbsf, which contains significant chert. Stratigraphic markers across the Eocene interval include polarity chrons (Ogg and Bardot, 2001), calcareous nannofossil biohorizons (Mita, 2001), and planktic foraminiferal biohorizons (Norris et al., 1998; Luciani and Giusberti, 2014). However, as first noted by Cramer et al. (2003), there is a basic stratigraphic problem with the labelling of the polarity chrons. The intervals of normal polarity between approximately 388 and 395 mbsf, and between approximately 412 and 420 mbsf were tentatively assigned to C22n and C23n, respectively (Ogg and Bardot, 2001). The original assignment was adopted by Luciani and Giusberti (2014), who considered the last occurrence of *Morozovella subbotinae* as happened near the top of C23n, according to Wade et al. (2011).

These age assignments, however, cannot be correct, because calcareous nannofossil biohorizons that lie below or within C22n (top of *T. orthostylus*, top of *Toweius*, base of *D. sublodoensis*) occur above 388 mbsf (Mita, 2001). Instead, there must be a significant hiatus or condensed interval at the chert horizon, and the intervals of normal polarity are C23n and C24n.1n.

4 Methods

4.1 Samples for isotopes and foraminifera

The three sites provide a good stratigraphic background and key existing data for understanding the temporal link between the EECO, carbon isotope perturbations and planktic foraminiferal evolution. Our analytical aim was to obtain comparable data sets across the sites. More specifically, a need existed to generate stable isotope and planktic

foraminiferal assemblage records at the Possagno section, to generate stable isotope records at DSDP Site 577, and to generate planktic foraminifera assemblage records at ODP Site 1051.

A total of 298 samples were collected from the Possagno section in 2002-2003 for isotope analyses. The sampling interval was 2 to 5 cm for the basal 0.7 m, 50 cm, and 20 cm for the interval between 0.7 m and 66 m. Bulk sediment samples previously were examined for their calcareous nannofossil assemblages (Agnini et al., 2006). One hundred and ten samples were selected for the foraminiferal study.

Aliquots of the 110 samples were weighed, and then washed to obtain foraminifera using two standard procedures, depending on lithology. For the indurated marly limestones and limestones, the cold-acetolyse technique was used (Lirer, 2000; Luciani and Giusberti, 2014). This method disaggregates strongly lithified samples, in which foraminifera otherwise can be analyzed only with thin sections (Fornaciari et al., 2007; Luciani et al., 2007). For the marls, samples were disaggregated using 30 % hydrogen peroxide and subsequently washed and sieved at 63 μm. In most cases, gentle ultrasonic treatment (e.g., low-frequency at 40 kHz for 30–60 seconds) improved the cleaning of the tests.

Relative abundance data of planktic foraminiferal samples were generated for 65 samples at Site 577 (Lu, 1995; Lu and Keller, 1995). We collected new samples spanning their effort for stable isotopes (below).

Fifty samples of Eocene sediment were obtained from Hole 1051A between 452 to 353 mbsf. Sample spacing varied from 2.0 m to 0.5 m. As the samples are ooze and chalk, they were prepared using disaggregation using distilled water and washing over 38 μm and 63 μm sieves. Washed residues were dried at <50°C.

4.2 Stable Isotopes

Carbon and oxygen stable isotope data of bulk sediment samples from the Possagno section and Site 577 were analysed using a Finnigan MAT 252 mass spectrometer equipped with a Kiel device at Stockholm University. Precision is within ±0.06 ‰ for carbon isotopes and within ±0.07 ‰ for oxygen isotopes. Stable isotope values were calibrated to the Vienna Pee Dee Belemnite standard (VPDB) and converted to conventional delta notation ($\delta^{13}C$ and $\delta^{18}O$).

4.3 Foraminifera analyses

The weight percent of the >63 μm size fraction relative to the weight of the bulk sample, typically 100 g/sample was calculated for the 110 Possagno samples. This is referred to as the coarse fraction, following previous work (Hancock and Dickens, 2005). Due to the consistent occurrence of radiolarians at Site 1051, the coarse fraction cannot give information on foraminiferal productivity.

Relative abundances for both Possagno and Site 1051 have been determined from about 300 complete specimens extracted from each of the 110 samples investigated in the >63 μm size fraction from random splits.

The degree of dissolution, expressed as the fragmentation index (*F* index) was evaluated according to Petrizzo et al. (2008) on ca. 300 elements, by counting planktic foraminiferal fragments or partially dissolved tests versus complete tests. These data are expressed in percentages. Fragmented foraminifera include specimens showing missing chambers and substantial breakage. The taxonomic criteria for identifying planktic foraminifera follows the work by Pearson et al. (2006).

5 Results

5.1 Carbon isotopes

Possagno

Carbon isotopes of bulk carbonate at Possagno vary between +1.8 and -0.3 ‰ (**Figure 4, Table S1**). Overall, $d^{13}C$ decreases from 1.8 ‰ at the base of the section to about 0.6 ‰ at 14 m. Generally, values then increase to 1.5 ‰ at 24 m, and remain between 1.5 ‰ and 0.8 ‰ for the remainder of the studied interval.

Superimposed on these trends are a series of negative CIEs. The most prominent of these (~1.5 ‰) occurs at the 0 m level, and marks the PETM (Agnini et al., 2009). However, at least ten additional negative CIEs lie above this marker and within the lowermost 21.4 m (**Figure 4, Table S1**). The lower two at ~8 m and ~12.5 m probably represent the H-1/ETM-2 and J event, respectively, as they lie at the appropriate stratigraphic horizons in relation to polarity chrons. The K/X event may lie at 14.8 m, although this height marks the start of the condensed interval.

The complex interval between 15.5 m and 24 m broadly corresponds to all of Chron C23n and the bottom half of Chron C22r. A series of CIEs occur in that interval on the order of 1.4 ‰, superimposed on a background trend of increasing $\delta^{13}C$ values (about 0.7 ‰). We tentatively label these CIEs with even numbers for internal stratigraphic purposes (**Figure 4**), as will become obvious below; their magnitudes range between 0.9 and 0.3 ‰ (**Table S1**). However, the sample spacing through this interval varies from 20 to 50 cm. The precise magnitudes and positions certainly could change with higher sample resolution, given the estimated compacted sedimentation rate of ~0.5 cm/kyr for this part of the section (Agnini et al., 2006).

344 Above Chron C22r, the Possagno $d^{13}C$ record contains additional minor CIEs (**Figure 4**).
345 The most prominent of these CIEs, at least relative to baseline values (~1.2 ‰), occurs within
346 Chron C21n. More important to understanding the EECO, a ~0.6 ‰ CIE nearly coincides
347 with the base of *D. sublodoensis* within the lower part of Chron C22n.
348
349 *DSDP Site 577*
350 The $d^{13}C$ record of bulk carbonate at DSDP Site 577 from just prior to the PETM through
351 Chron C22n ranges between 2.3 and 0.6 ‰ (**Figure 5; Table S2**). Overall, $d^{13}C$ decreases
352 from 1.4 ‰ at 84.5 mcd to about 0.6 ‰ at ~76 mcd. Values then generally increase to 2.1 ‰
353 at ~68 mcd, and remain between 2.3 ‰ and 1.6 ‰ for the rest of the studied interval. Thus,
354 the ranges and general trends in $d^{13}C$ for the two sections are similar, but skewed at DSDP
355 Site 577 relative to Possagno by about +0.6 ‰.
356 Like at Possagno, the early Eocene $\delta^{13}C$ record at DSDP Site 577 exhibits a series of
357 CIEs (**Figure 5**). The portion of this record from the PETM through the K/X event has been
358 documented and discussed elsewhere (Cramer et al., 2003; Dickens and Backman, 2013). The
359 new portion of this record, from above the K/X event through Chron C22n, spans the
360 remainder of the EECO. Within this interval, where background $\delta^{13}C$ values rise by ~1.5 ‰,
361 there are again a series of minor CIEs with magnitudes between 0.3 and 0.5 ‰ (**Table S2).**
362 We again give these an internal numerical labelling scheme. A ~0.4 ‰ CIE also nearly
363 coincides with the base of *D. sublodoensis* within the lower part of C22n.
364
365 **5.2 Oxygen isotopes**
366
367 *Possagno*
368 Oxygen isotopes of bulk carbonate at Possagno range between -3.3 and 0.8 ‰ with a mean

value of -1.7 ‰ (**Figure 4, Table S1**). In general, there exists considerable scatter, with adjacent samples often having a $\delta^{18}O$ difference exceeding 0.5 ‰. Nonetheless, some of the more prominent decreases in $\delta^{18}O$ show a clear correspondence with negative $\delta^{13}C$ values (CIEs) and vice versa. This correspondence occurs across the PETM and other known hyperthermals, as well as within and after the EECO. Indeed, the main phase of the EECO appears to correspond with a broad low in $d^{18}O$.

DSDP Site 577

The $\delta^{18}O$ record at Site 577 noticeably deviates from that at Possagno (**Figure 5, Table S2**). This is because values range between 0.2 and -1.1 ‰ with an average value of -0.4 ‰. Thus, both records have somewhat similar scatter, but the Possagno record is shifted overall by about -1.3 ‰ relative to that at Site 577. There is again a modest correlation between decreases in $\delta^{18}O$ and negative $\delta^{13}C$ values, as well as a general low in $\delta^{18}O$ across the main phase of the EECO.

5.3 Coarse fraction

The coarse fraction of samples from Possagno shows two distinct trends (**Figure 6, Table S3**). Before the EECO, values are 10.4 % ± 2.67 %. However, from the base of the EECO and up through the section, values decrease to 5.3 ± 1.3 %.

5.4 Foraminiferal preservation and fragmentation

Planktic foraminifera are consistently present and diverse throughout the studied intervals at Possagno and at ODP Site 1051. Preservation of the tests at Possagno varies from moderate

394 to fairly good (Luciani and Giusberti, 2014). However, planktic foraminifera tests at
395 Possagno are recrystallized and essentially totally filled with calcite. Planktic foraminifera
396 from samples at Site 1051 are well preserved throughout the studied interval. Planktic
397 foraminifera from Site 577, at least as illustrated by published plates (Lu and Keller, 1995),
398 show a very good state of preservation.

399 The *F* index record at Possagno (**Figure 6, Table S3**) displays large amplitude variations
400 throughout the investigated interval. The highest values, up to 70 %, were observed between
401 16 and 22 m. In general, highs in *F* index values correspond to lows in the $\delta^{13}C$ record.

402 The *F* index record at Site 1051 (**Figure 7, Table S4**) shows less variability compared to
403 that at Possagno, although some of this may reflect the difference in the number of samples
404 examined at the two locations. A maximum value of 60 % is found in Zone E5, just below an
405 interval of uncertain magnetostratigraphy (Norris et al., 1998), but corresponding to the J
406 event (Cramer et al., 2003). Relatively high *F* index values, around 50 %, also occur in
407 several samples below this horizon. The interval across the EECO generally displays low *F*
408 index values (<20 %).

409

410 **5.5 Planktic foraminiferal quantitative analysis**

411

412 *Possagno*

413 Planktic foraminiferal assemblages at Possagno show significant changes across the early to
414 early middle Eocene (**Figure 6, Table S3**). Throughout the entire section, the mean relative
415 abundance of *Acarinina* is about 46 % of the total assemblage. However, members of this
416 genus show peak abundances of 60-80 % of the total assemblage occur across several
417 intervals, often corresponding to CIEs. Particularly prominent is the broad abundance peak of
418 *Acarinina* coincident with the main phase of the EECO.

419 The increases in acarininid relative abundance typically are counterbalanced by transient
420 decreases of subbotinids (**Figure 6**). This group also shows a general increase throughout the
421 section. Below the EECO the relative abundances of subbotinids average ~24 %. Above the
422 EECO, this average rises to ~36 %.
423 The trends of acarininids and subbotinids contrast with that of morozovellids (**Figure 6**),
424 which exhibit a major and permanent decline within Zone E5. This group collapses from
425 mean abundances ~24 % in the 0-15 m interval to <6 % above 15 m. Qualitative examination
426 of species shows that, in the lower part of Zone E5, where relatively high morozovellids
427 abundances are recorded, there is no dominance of any species. *M. marginodentata*, *M.*
428 *subbotinae* and *M. lensiformis* are each relatively common, and *M. aequa, M. aragonensis*,
429 *M. formosa* and *M. crater* are each less common. By contrast, in the upper part of Zone E5,
430 where low morozovellids abundances occur, *M. aragonensis, M. formosa, M. crater* and *M.*
431 *caucasica* are the most common species. The general decrease of morozovellids abundances
432 appears unrelated to the disappearance of a single, dominant species.
433 At Possagno, morozovellids never recover to their pre-EECO abundances. This is true
434 even if one includes the morphologically and ecologically comparable genus *Morozovelloides*
435 (Pearson et al., 2006), which first appears in samples above 36 m.
436 Other planktic foraminifera genera are always less than 15 % of the total assemblages
437 throughout the studied interval at Possagno (**Figure S1, Table S3**).
438
439 *ODP Site 577*
440 Samples from Site 577 were disaggregated in water and washed through a >63 sieve (Lu,
441 1995; Lu and Keller, 1995). They determined relative abundances of planktic foraminifera
442 from random splits of about 300 specimens (Lu, 1995; Lu and Keller, 1995). The resulting
443 data are shown in **Figure 7**, placed onto the composite depth scale by Dickens and Backman

(2013). Major changes in planktic foraminiferal assemblages are comparable to those recorded at Possagno. Such changed include indeed a distinct decrease of morozovellids within Zone E5. The decrease at Site 577 is from mean values of 26.6 % to 6.7 % (**Table S4**). This marked drop occurs at ca. 78 mcd close to the J event and at the start of the EECO. Like at Possagno, morozovellids never recover to their pre-EECO abundances.

The morozovellids decrease is counter balanced by the trend of acarininids abundances that increase from mean values of 30.4 % to 64.8 % in correspondence to the level of the morozovellids collapse. Subbotinids fluctuate in abundance throughout the interval investigated from 1 % to 18 %, with a mean value of ca. 8 %.

ODP Site 1051

Planktic foraminifera show distinct changes in abundance at Site 1051 (**Figure 8, Table S5**). The changes of the main taxa are similar to the variations observed at Possagno. The genus *Acarinina* displays an increase in mean relative abundance from 35 % (base to ca. 450 mbsf) to around 50 % (ca. 430 mbsf), with maximum values of about 60 %. The relatively low resolution used here does not permit comparison to the early Eocene CIEs at Site 1051 (Cramer et al., 2003), or how the relative abundance of planktic foraminiferal genera varies with respect to CIEs.

The abundance of subbotinids shows little variations around mean values of 20 % at Site 1051. Like at Possagno, samples from Site 1051 also record a slight increase above the EECO (ca. 7 %, mean value).

The major change in planktic foraminiferal assemblages at Site 1051 includes a distinct decrease of *Morozovella*, from mean values around 40 % to 10 % in the middle part of Zone E5 (**Figure 7**). Similar to Possagno, the lower part of Zone E5 with the higher percentages of morozovellids does not record the dominance of selected species, but at Site 1051 *M.*

aragonensis and *M. formosa* besides *M. subbotinae* are relatively common whereas *M. marginodentata* is less frequent. Within the interval of low morozovellids abundances, *M. aragonensis* and *M. formosa* are the most common taxa. The general decline of morozovellids does not appear therefore related, both at Possagno and Site 1051, to the extinction or local disappearance of a dominant species.

6 Discussion

6.1 Dissolution, recrystallization, and bulk carbonate stable isotopes

The bulk carbonate stable isotope records within the lower Paleogene sections at Possagno and at Site 577 need consideration as to how such records are produced and modified in much younger strata dominated by pelagic carbonate. In open ocean environments, carbonate preserved on the seafloor principally consists of calcareous tests of nannoplankton (coccolithophores) and planktic foraminifera (Bramlette and Riedel, 1954; Berger, 1967; Vincent and Berger, 1981). However, the total amount of carbonate and its microfossil composition can vary considerably across locations because of differences in deep-water chemistry and in test properties (e.g., ratio of surface area to volume; mineralogical composition). For regions at low to mid latitudes, a reasonable representation of carbonate components produced in the surface water accumulates on the seafloor at modest (<2000 m) water depth. By contrast, microfossil assemblages become heavily modified in deeper water, because of increasingly significant carbonate dissolution (Berger, 1967). Such dissolution preferentially affects certain tests, such as thin-walled, highly porous planktic foraminifera (Berger, 1970; Bé et al., 1975; Thunell and Honjo, 1981).

The stable isotope composition of modern bulk carbonate ooze reflects the mixture of its

carbonate components, which mostly record water temperature and the composition of dissolved inorganic carbon (DIC) within the mixed layer (<100 m water depth). The stable isotope records are imperfect, though, because of varying proportions of carbonate constituents, and "vital effects", which impact stable isotope fractionation for each component (Anderson and Cole, 1975; Reghellin et al., 2015). Nonetheless, the stable isotope composition of bulk carbonate ooze on the seafloor can be related to overlying temperature and chemistry of surface water (Anderson and Cole, 1975; Reghellin et al., 2015).

Major modification of carbonate ooze occurs during sediment burial. This is because, with compaction and increasing pressure, carbonate tests begin to dissolve and recrystallize (Schlanger and Douglas, 1974; Borre and Fabricus, 1998). Typically within several hundred meters of the seafloor, carbonate ooze becomes chalk and, with further burial, limestone (Schlanger and Douglas, 1974; Kroencke et al., 1991; Borre and Fabricus, 1998). Carbonate recrystallization appears to be a local and nearly closed system process, such that mass transfer occurs over short distances (i.e., less than a few meters) (above references and Matter et al., 1975; Arthur et al., 1984; Frank et al., 1999).

In pelagic sequences with appreciable carbonate content, bulk carbonate $\delta^{13}C$ records typically give information of paleoceanographic significance (Scholle and Arthur, 1980; Frank et al., 1999). Even when transformed to indurated limestone, the $\delta^{13}C$ value for a given sample should be similar to that originally deposited on the seafloor. This is because almost all carbon within small sedimentary volumes exists as carbonate. Bulk carbonate $\delta^{18}O$ records are a different matter, especially in indurated marly limestones and limestones (Marshall, 1992; Schrag et al., 1995; Frank et al., 1999). This is because pore water dominates the total amount of oxygen within an initial parcel of sediment, and oxygen isotope fractionation depends strongly on temperature. Thus, during dissolution and recrystallization of carbonate, significant exchange of oxygen isotopes occurs. At first, carbonate begins to preferentially

519 acquire ^{18}O, because shallowly buried sediment generally has colder temperatures than
520 surface water. However, with increasing burial depth along a geothermal gradient, carbonate
521 begins to preferentially acquire ^{16}O (Schrag et al., 1995; Frank et al., 1999).
522
523 **6.2 Carbon isotope stratigraphy through the EECO**
524
525 Stratigraphic issues complicate direct comparison of various records from Possagno and Site
526 577. The two sections have somewhat similar multi-million year sedimentation rates across
527 the early Eocene. However, the section at Possagno contains the condensed interval, where
528 much of C23r spans a very short distance (Agnini et al., 2006), and the section at Site 577 has
529 a series of core gaps and core overlaps (Dickens and Backman, 2013).
530 An immediate issue to amend is the alignment of Cores 8H and 9H in Hole 577* and
531 Core 8H in Hole 577A (**Figure 5**). On the basis of GRAPE density records for these cores,
532 Dickens and Backman (2013) initially suggested a 2.6 m core gap between Cores 8H* and
533 9H*. However, a 3.5 m core gap also conforms to all available stratigraphic information. The
534 newly generated $\delta^{13}C$ (and $\delta^{18}O$) records across these three cores show the latter to be correct.
535 Once sedimentation rate differences at Possagno are recognized and coring problems at
536 Site 577 are rectified, early Eocene $\delta^{13}C$ records at both locations display similar trends and
537 deviations in relation to polarity chrons and key microfossil events (**Figures 4, 5**). Moreover,
538 the $\delta^{13}C$ variations can be correlated in time to those found in bulk carbonate $\delta^{13}C$ records at
539 other locations, including Site 1051 (**Figure 8**) and Site 1258 (**Figure 9**). As noted
540 previously, such correlation occurs because the bulk carbonate $\delta^{13}C$ signals reflect past global
541 changes in the composition of surface water DIC, even after carbonate recrystallization.
542 For the latest Paleocene and earliest Eocene, nominally the time spanning from the base
543 of C24r through the middle of C24n, detailed stable carbon isotope records have been

544 generated at more than a dozen locations across the globe (Cramer et al., 2003; Agnini et al.,
545 2009; Galeotti et al., 2010; Zachos et al., 2010; Slotnick et al., 2012; Littler et al., 2014;
546 Agnini et al., in review). These records can be described consistently as a long-term drop in
547 $\delta^{13}C$ superimposed with a specific sequence of prominent CIEs that include those
548 corresponding to the PETM, H-1, and J events. In continuous sections with good
549 magnetostratigraphy and biostratigraphy, there is no ambiguity in the assignment of CIEs
550 (Zachos et al., 2010; Littler et al., 2014; Slotnick et al., 2012, 2105a; Lauretano et al., 2015).
551 This "$\delta^{13}C$ template" can be found at the Possagno section and at Site 577 (**Figure 9**); it is
552 found at Site 1051 for the depth interval where carbon isotopes have been determined
553 (**Figure 8**).
554 After the J event and across the EECO, very few detailed $\delta^{13}C$ records have been
555 published (Slotnick et al., 2012, 2015a; Kirtland-Turner et al., 2014). Moreover, the available
556 records are not entirely consistent. For example, the K/X event in Clarence River valley
557 sections manifests as a prominent CIE within a series of smaller $\delta^{13}C$ excursions (Slotnick et
558 al., 2012, 2015a), whereas the event has limited expression in the $\delta^{13}C$ record at Site 1258
559 (Kirtland-Turner et al., 2014; **Figure 9**).
560 The new records from Possagno and Site 577 emphasize an important finding regarding
561 bulk carbonate $\delta^{13}C$ records across the EECO. Between the middle of C24n and the upper
562 part of C23r, there appears to be a sequence of low amplitude, low frequency CIEs. (Note
563 that this portion of the record is missing at Possagno because of the condensed interval;
564 **Figure 9**). However, near the C23r/C23n boundary, a long-term rise in $\delta^{13}C$ begins, but with
565 a series of relatively high amplitude, high frequency CIEs (Kirtland-Turner et al., 2014;
566 Slotnick et al., 2014). The number, relative magnitude and precise timing of CIEs within this
567 interval remain uncertain. For example, the CIE labelled "4" appears to occur near the top of
568 C23r at Site 577 but near the bottom of C23n.2n at Site 1258 and at Possagno. Additional

569 $\delta^{13}C$ records across this interval are needed to resolve the correct sequence of CIEs and to
570 derive an internally consistent labelling scheme for these perturbations. It is also not clear
571 which of these CIEs during the main phase of the EECO specifically relate to significant
572 increases in temperature, as clear for the "hyperthermals" in the earliest Eocene. Nonetheless,
573 numerous CIEs, as well as an apparent change in the mode of these events, characterize the
574 EECO (Kirtland-Turner et al., 2014; Slotnick et al., 2014).

575 The causes of $\delta^{13}C$ changes during the early Paleogene lie at the crux of considerable
576 research and debate (Dickens et al., 1995, 1997; Zeebe et al., 2009; Dickens, 2011; Lunt et
577 al., 2011; Sexton et al., 2011; De Conto et al., 2012; Lee et al., 2013; Kirtland Turner et al.,
578 2014). Much of the discussion has revolved around three questions: (1) what are the sources
579 of ^{13}C-depleted carbon that led to prominent CIEs, especially during the PETM? (2) does the
580 relative importance of different carbon sources vary throughout this time interval? and, (3)
581 are the geologically brief CIEs related to the longer secular changes in $\delta^{13}C$? One might
582 suggest, through several papers, a convergence of thought as to how carbon cycled across
583 Earth's surface during the early Paleogene, at least between the late Paleocene and the K/X
584 event (Cramer et al., 2003; Lourens et al., 2005; Galeotti et al., 2010; Hyland et al., 2013;
585 Zachos et al., 2010; Lunt et al. 2011; Littler et al., 2014; Lauretano et al., 2015; Westerhold et
586 al., 2015). Changes in tectonics, volcanism, and weathering drove long-term changes
587 atmospheric pCO_2 (Vogt, 1979; Raymo and Ruddiman, 1992; Sinton and Duncan, 1998;
588 Demicco, 2004; Zachos et al., 2008), which was generally high throughout the early
589 Paleogene, but increased toward the EECO (Pearson and Palmer, 2000; Fletcher et al., 2008;
590 Lowenstein and Demicco, 2006; Smith et al., 2010; Hyland and Sheldon, 2013). However, as
591 evident from the large range in $\delta^{13}C$ across early Paleogene stable isotope records, major
592 changes in the storage and release of organic carbon must have additionally contributed to
593 variability in atmospheric pCO_2 and ocean DIC concentrations (Shackleton, 1986; Kurtz et

al., 2003; Komar et al., 2013). When long-term increases in pCO_2, perhaps in conjunction with orbital forcing, pushed temperatures across some threshold, such as the limit of sea-ice formation (Lunt et al., 2011), rapid inputs of ^{13}C-depleted organic carbon from the shallow geosphere served as a positive feedback to abrupt warming (Dickens et al., 1995; Bowen et al., 2006; DeConto et al., 2012).

Our new $\delta^{13}C$ records do not directly address the above questions and narrative concerning early Paleogene carbon cycling. However, they do highlight two general and related problems when such discussion includes the EECO. First, surface temperatures appear to stay high across an extended time interval when the $\delta^{13}C$ of benthic foraminifer (**Figure 1**) and bulk carbonate (**Figure 9**) increase. Second, numerous brief CIEs mark this global long-term rise in $\delta^{13}C$. Whether the aforementioned views need modification or reconsideration (Kirtland Turner et al., 2014) is an outstanding issue, one that depends on how long-term and short-term $\delta^{13}C$ changes relate across the entire early Paleogene.

The overall offset between bulk carbonate $\delta^{13}C$ values at Possagno and Site 577 may hint at an important constraint to any model of early Paleogene carbon cycling. Throughout the early Eocene, $\delta^{13}C$ values at Site 577 exceed those at Possagno by nominally 0.8 ‰ (**Figure 9**). This probably does reflect recrystallization or lithification, because similar offsets appear across numerous records independent of post-depositional history but dependent on location (Cramer et al., 2003; Slotnick et al., 2012, 2015a). In general, absolute values of bulk carbonate $\delta^{13}C$ records increase from the North Atlantic through the South Atlantic, Indian and Pacific oceans.

6.3 Stable oxygen isotope stratigraphy across the EECO

Bulk carbonate $\delta^{18}O$ values for Holocene sediment across the Eastern Equatorial Pacific

619 relate to average temperatures in the mixed layer (Shackleton and Hall, 1995; Reghellin et al.,
620 2015). Indeed, values are close to those predicted from water chemistry ($\delta^{18}O_w$) and
621 equilibrium calculations for calcite precipitation (e.g., Bemis et al., 1998) if vital effects in
622 the dominant nannoplankton increase $\delta^{18}O$ by nominally 1‰ (Reghellin et al., 2015).
623 Site 577 was located at about 15°N latitude in the eastern Pacific during the early
624 Paleogene. Given that sediment of this age remains "nannofossil ooze" (Shipboard Scientific
625 Party, 1985), one might predict past mixed layer temperatures from the $\delta^{18}O$ values with
626 three assumptions: early Paleogene $\delta^{18}O_w$ was 1.2 ‰ less than that at present-day to account
627 for an ice-free world; local $\delta^{18}O_w$ was equal to average seawater, similar to modern chemistry
628 at this off-Equator location (LeGrande and Schmidt, 2006); and, Paleogene nannoplankton
629 also fractionated $\delta^{18}O$ by 1.0 ‰. With commonly used equations that relate the $\delta^{18}O$ of
630 calcite to temperature (Bemis et al., 1998), these numbers render temperatures of between
631 16°C and 21°C for the data at Site 577. Such temperatures seem too cold by at least 10°C,
632 given other proxy data and modelling studies (e.g., Huber and Caballero, 2011; Hollis et al.,
633 2012; Pross et al., 2012; Inglis et al., 2015).
634 At low latitudes, bottom waters are always much colder than surface waters. Even during
635 the EECO, deep waters probably did not exceed 12°C (Zachos et al., 2008). The calculated
636 tepid temperatures likely indicate partial recrystallization of bulk carbonate near the seafloor.
637 Examinations of calcareous nannofossils in Paleogene sediment at Site 577 show extensive
638 calcite overgrowths (Shipboard Scientific Party, 1985; Backman, 1986). Relatively low $\delta^{18}O$
639 values mark the H-1 and K/X events, as well as the main phase of the EECO (**Figure 5**). Both
640 observations support the idea that the bulk carbonate $\delta^{18}O$ at Site 577 represents the
641 combination of a primary surface water $\delta^{18}O$ signal and a secondary shallow pore water $\delta^{18}O$
642 signal.
643 Lithification should further impact bulk carbonate $\delta^{18}O$ records (Marshall, 1992; Schrag

644 et al., 1995; Frank et al., 1999). Because this process occurs well below the seafloor, where
645 temperatures approach or exceed those of surface water, the $\delta^{18}O$ values of pelagic marls and
646 limestones should be significantly depleted in ^{18}O relative to partially recrystallized
647 nannofossil ooze. This explains the nominal 2 ‰ offset in average $\delta^{18}O$ between correlative
648 strata at Possagno and Site 577. While temperature calculations using the $\delta^{18}O$ record at
649 Possagno render reasonable surface water values for a mid-latitude location in the early
650 Paleogene (26-31°C, using the aforementioned approach), any interpretation in these terms
651 likely reflects happenstance. The fact that planktic foraminifera are completely recrystallized
652 and totally filled with calcite at this site supports this inference.
653 As observed at Site 577, however, horizons of lower $\delta^{18}O$ at Possagno may represent
654 times of relative warmth in surface water. This includes the broad interval between 16 and
655 22.5 m, which marks the main phase of the EECO, as well as many of the brief CIEs, at least
656 one that clearly represents the PETM (**Figure 4**). That is, despite obvious overprinting of the
657 original $\delta^{18}O$ signal, early to early middle Eocene climate variations appear manifest in the
658 data.
659
660 **6.4 The EECO and planktic foraminiferal abundances**
661
662 Bulk carbonate $\delta^{13}C$ records, especially in conjunction with other stratigraphic markers,
663 provide a powerful means to correlate early Paleogene sequences from widely separated
664 locations (**Figure 9**). They also allow for placement of planktic foraminiferal assemblage
665 changes into broader context.
666 The most striking change in planktic foraminiferal assemblages occurred near the start of
667 the EECO. Over a fairly short time interval and at multiple widespread locations, the relative
668 abundance of acarininids increased significantly whereas the relative abundance of

669 morozovellids decreased significantly. This switch, best defined by the decline in
670 morozovellids, happened just before the condensed interval at Possagno (**Figure 6**), just
671 above the J event at Site 577 (**Figure 7, Table S4**), and during the J event at Site 1051
672 (**Figure 8**). At the Farra section, cropping out in the same geological setting of Possagno at
673 50 km NE of the Carcoselle quarry, it also appears to have occurred close to the J event
674 (**Figure 10**). Indeed, the maximum turnover in relative abundances may have been coincident
675 with the J event at all locations. Importantly, the relative abundance of subbotinids only
676 changed marginally during this time.
677 The "morozovellids crisis" across the start of the EECO was irreversible. At Possagno
678 and at Site 1051, it was coupled with the gradual disappearances of several species, including
679 *M. aequa, M. gracilis, M. lensiformis, M. marginodentata,* and *M. subbotinae*. Furthermore,
680 the loss of morozovellids was not counterbalanced by the appearance of the *Morozovelloides*
681 genus, which shared with *Morozovella* the same ecological preferences. This latter genus
682 appeared in C21r, near the Ypresian/Lutetian boundary, and well after the EECO (Pearson et
683 al., 2006; Aze et al., 2011), including at Possagno (Luciani and Giusberti, 2014; **Figure 6**).
684 Though *Morozovelloides* were morphologically similar to *Morozovella*, they probably
685 evolved from *Acarinina* (Pearson et al., 2006).
686 At Possagno, higher abundances of acarininids also correlate with the pronounced
687 negative $\delta^{13}C$ perturbations before and after the EECO (**Figure 6**). This includes the H-1
688 event, as well as several unlabelled CIEs during C22n, C21r and C21n. Such increases in the
689 relative abundances of acarininids have been described for the PETM interval at the proximal
690 Forada section (Luciani et al., 2007), and for the K/X event at the proximal Farra section
691 (Agnini et al., 2009). Unlike for the main switch near the J event, however, these changes are
692 transient, so that relative abundances in planktic foraminiferal genera are similar before and
693 after the short-term CIEs.

694

695 **6.5 The impact of dissolution**

696

697 Carbonate dissolution at or near the seafloor presents a potential explanation for observed
698 changes in foraminifera assemblages. Some studies of latest Paleocene to initial Eocene age
699 sediments, including laboratory experiments, suggest a general ordering of dissolution
700 according to genus, with acarininds more resistant than morozovellids, and the latter more
701 resistant than subbotinids (Petrizzo et al., 2008; Nguyen et al., 2009, 2011).

702 Carbonate solubility horizons that impact calcite preservation and dissolution on the
703 seafloor (i.e., the CCD and lysocline) also shoaled considerably during various intervals of
704 the early Eocene. The three most prominent hyperthermals that occurred before the main
705 phase of the EECO (PETM, H-1, K/X) were clearly marked by pronounced carbonate
706 dissolution at multiple locations (Zachos et al., 2005; Agnini et al., 2009; Stap et al., 2009;
707 Leon-Rodriguez and Dickens, 2010). A multi-million year interval characterized by a
708 relatively shallow CCD also follows the K/X event (Leon-Rodriguez and Dickens, 2010;
709 Pälike et al., 2012; Slotnick et al., 2015b).

710 Should changes in carbonate preservation primarily drive the observed planktic
711 foraminiferal assemblages, it follows that the dominance of acarininids during the EECO and
712 multiple CIEs could represent a taphonomic artefact. Limited support for this idea comes
713 from our records of fragmentation (*F* index). In general, intervals with relatively high
714 abundances of acarininids (and low $\delta^{13}C$) correspond to intervals of fairly high fragmentation
715 at Possagno and at Site 1051 (**Figures 6, 8**). This can suggest carbonate dissolution, because
716 this process breaks planktic foraminifera into fragments (Berger, 1967; Hancock and
717 Dickens, 2005).

718 Carbonate dissolution can cause the coarse fraction of bulk sediment to decrease (Berger

et al., 1982; Broecker et al., 1999; Hancock and Dickens, 2005). This happens because whole planktic foraminiferal tests typically exceed 63 μm, whereas the resulting fragments often do not exceed 63 μm. The decrease in CF values at the start of the EECO at Possagno (**Figure 6**) may therefore further indicate loss of foraminiferal tests. However, relatively low CF values continue to the top of the section, independent of changes in the *F* index. The CF record parallels the trend of morozovellids abundance, and thus might also suggest a loss of larger morozovellids rather than carbonate dissolution.

The cause of the long-term rise in carbonate dissolution horizons remains perplexing, but may relate to reduced inputs of ^{13}C-depleted carbon into the ocean and atmosphere (Leon-Rodriguez and Dickens, 2010; Komar et al., 2013). Should the morozovellids decline and amplified *F* index at the Possagno section mostly represent dissolution, it would imply considerable shoaling of these horizons in the western Tethys, given the inferred deposition in middle to lower bathyal setting. As with open ocean sites (Slotnick et al., 2015b), further studies on the Eocene CCD are needed from Tethyan locations. One idea is that remineralization of organic matter intensified within the water column, driven by augmented microbial metabolic rates at elevated temperatures during the EECO; this may have decreased pH at intermediate water column depths (Brown et al., 2004; Olivarez Lyle and Lyle, 2006; O'Connor et al., 2009; John et al., 2013, 2014).

Despite evidence for carbonate dissolution, this process probably only amplified primary changes in planktic foraminifera assemblages. The most critical observation is the similarity of the abundance records for major planktic foraminiferal genera throughout the early Eocene at multiple locations (**Figures 6-8**). This includes the section at Site 1051, where carbonate appears only marginally modified by dissolution according to the *F* index values (**Figure 7**). Subbotinid abundance also remains fairly high throughout the early Eocene. One explanation is that, in contrast to laboratory experiments (Nguyen et al., 2009, 2011), subbotinids are

744 more resistant to dissolution than morozovellids (Boersma and Premoli Silva, 1983; Berggren
745 and Norris, 1997), at least once the EECO has transpired. In the proximal middle-upper
746 Eocene section at Alano, Luciani et al. (2010) documented a dominance of subbotinids within
747 intervals of high fragmentation (*F* index) and enhanced carbonate dissolution. The degree of
748 dissolution across planktic foraminiferal assemblages may have varied through the early
749 Paleogene, as distinct species within each genus may respond differently (Nguyen et al.,
750 2011). So far, data on dissolution susceptibility for different species and genera are lacking
751 for early and early middle Eocene times.
752 There is also recent work from the Terche section (ca. 28 km NE of Possagno) to
753 consider. This section is located in the same geological setting as Possagno, but across the H-
754 1, H-2 and I1 events, there are very low *F* index values and marked increases of acarininids
755 coupled with significant decreases of subbotinids (D'Onofrio et al., 2014). Therefore,
756 although the Possagno record may be partially altered by dissolution, an increase of warm
757 water acarininids concomitant with decrease of subbotinids seems to be a robust finding
758 during early Paleogene warming events in Tethyan settings.
759
760 **6.6 A record of mixed water change**
761
762 The switch in abundance between morozovellids and acaraninids at the start of the EECO
763 supports a hypothesis whereby environmental change resulted in a geographically widespread
764 overturn of planktic foraminifera genera. During the PETM and K/X events, acarininids
765 became dominant over morozovellids in a number of Tethyan successions of northeast Italy.
766 This has been interpreted as signifying enhanced eutrophication of surface waters near
767 continental margins (Agnini et al., 2009; Arenillas et al., 1999; Luciani et al., 2007; Molina et
768 al., 1999), an idea consistent with evidence for elevated (albeit more seasonal) riverine

769 discharge during these hyperthermals (Schmitz and Pujalte, 2007; Giusberti et al., 2007;
770 Slotnick et al., 2012; Puljalte et al., 2015). Increased nutrient availability may also have
771 occurred at Possagno during the early part of the EECO, given the relatively high
772 concentration of radiolarians, which may reflect eutrophication (Hallock, 1987).
773 However, the fact that the major switch at the start of the EECO can be found at Sites
774 1051 (western Atlantic) and Site 577 (central Pacific) suggests that local variations in
775 oceanographic conditions, such as riverine discharge, was not the primary causal mechanism.
776 Rather, the switch must be a consequence of globally significant modifications related to the
777 EECO, most likely sustained high temperatures, elevated pCO_2, or both. Given model
778 predictions for our Earth in the coming millennia (IPCC, 2014), indirect effects also could
779 have contributed, especially including increased ocean stratification and decreased pH.
780 An explanation for the shift may lie in habitat differences across planktic foraminifera
781 genera. Although both morozovellids and acaraninids likely had photsymbionts,
782 morozovellids may have occupied a shallower surface habitat than the latter genus as
783 indicated by minor variations in their stable isotope compositions (Boersma et al., 1987;
784 Pearson et al., 1993; 2001).
785 One important consideration to any interpretation is the evolution of new species that
786 progressively appear during the post-EECO interval. In good agreement with studies of lower
787 Paleogene sediment from other low latitude locations (Pearson et al., 2006), thermocline
788 dwellers such as subbotinids and parasubbotinids seem to proliferate at Possagno (Luciani
789 and Giusberti, 2014). These include *Subbotina corpulenta, S. eocena, S. hagni, S. senni, S.*
790 *yeguanesis, Parasubbotina griffinae,* and *P. pseudowilsoni*. The appearance of the radially-
791 chambered *Parasubbotina eoclava*, considered to be the precursor of the truly clavate
792 chambered *Clavigerinella* (Coxall et al., 2003; Pearson and Coxall, 2014), also occurs at 19.8
793 m, and in the core of the EECO (Luciani and Giusberti, 2014). *Clavigerinella* is the ancestor

794 of the genus *Hantkenina* that successfully inhabited the sub-surface during the middle
795 through late Eocene.
796 A second consideration is the change in planktic foraminifera assemblages during the
797 Middle Eocene Climate Optimum (MECO), another interval of anomalous and prolonged
798 warmth ca. 40 Ma (Bohaty and Zachos, 2003). At Alano (**Figure 11**) and other locations
799 (Luciani et al., 2010; Edgar et al., 2012), the MECO involved the reduction in the abundance
800 and test size of large acarininids and *Morozovelloides*. This has been attributed to "bleaching"
801 and the loss of photosymbionts resulting from global warming (Edgar et al., 2012), although
802 related factors, such as a decrease in pH, a decrease in nutrient availability, or changes in
803 salinity, may have been involved (Douglas, 2003; Wade et al., 2008). The symbiotic
804 relationship with algae is considered an important strategy adopted by muricate planktic
805 foraminifera during the early Paleogene (Norris, 1996; Quillévéré et al., 2001). Considering
806 the importance of this relationship in extant species (Bé, 1982; Bé et al., 1982; Hemleben et
807 al., 1989), the loss of photosymbionts may represent a crucial mechanism to explain the
808 relatively rapid decline foraminifera utilizing this strategy, including morozovellids at the
809 start of the EECO.
810 Available data suggest that the protracted conditions of extreme warmth and high pCO_2
811 during the EECO were the key elements inducing a permanent impact on planktic
812 foraminiferal evolution, and the demise of the morozovellids. Even during the PETM, the
813 most pronounced hyperthermal, did not adversely affect the morozovellids permanently.
814 While "excursion taxa" appeared, morozovellids seem to have increased in abundance in
815 open ocean settings (Kelly et al., 1996; 1998, 2002; Lu and Keller, 1995; Petrizzo, 2007);
816 only in some continental margin settings did a transient decrease in abundance occur (Luciani
817 et al., 2007).
818

819 **6.7 Post-EECO changes at Possagno**

820

821 Several small CIEs appear in the $\delta^{13}C$ record at Possagno during polarity chrons C22n, C21r,
822 and C21n. Some of these post-EECO excursions coincide with planktic foraminiferal
823 assemblage changes similar to those recorded in lower strata. Specifically, there are marked
824 increases of acarininids (**Figure 6**). These "post-EECO" CIEs are concomitant with $\delta^{18}O$
825 excursions and coupled to distinct modifications in the planktic foraminiferal assemblages
826 comparable to those recorded across known hyperthermals in Tethyan settings (Luciani et al.,
827 2007; Agnini et al., 2009; D'Onofrio et al., 2014). Additional hyperthermals, although of less
828 intensity and magnitude, may extend through the entirety of the early and middle Eocene, as
829 suggested previously (Sexton et al., 2006; 2011; Kirtland-Turner et al., 2014). Whether these
830 imply different forcing and feedback mechanisms compared to the PETM remains an open
831 discussion.

832

833 **7 Summary and conclusions**

834 The symbiont-bearing planktic foraminiferal genera *Morozovella* and *Acarinina* were
835 among the most important calcifiers of the early Paleogene tropical and subtropical oceans.
836 However, a remarkable and permanent switch in the relative abundance of these genera
837 happened in the early Eocene, an evolutionary change accompanied by species reduction of
838 *Morozovella* and species diversification of *Acarinina*. We show here that this switch probably
839 coincided with a carbon isotope excursion (CIE) presently coined "J". Although the Early
840 Eocene Climatic Optimum (EECO), a multi-million year interval of extreme Earth surface
841 warmth, lacks an accepted definition, we agree with others that the EECO is best defined as
842 the duration of time between the "J event" and the base of *D. sublodoensis* (about 53 Ma to
843 49 Ma on the 2012 GTS).

844 Our conclusion that the planktic foraminferal switch coincides with the start of the
845 EECO derives from the generation of new records and collation of old records concerning
846 bulk sediment stable isotopes and planktic foraminiferal abundances at three sections. These
847 sections span a wide longitude range of the low latitude Paleogene world: the Possagno
848 section from the western Tethys, DSDP Site 577 from the central Pacific Ocean, and ODP
849 Site 1051 from the western Atlantic Ocean. Importantly, these locations have robust
850 calcareous nannofossils and polarity chron age markers, although the stratigraphy required
851 amendment at Sites 577 and 1051.
852 An overarching problem is that global carbon cycling was probably very dynamic during
853 the EECO. The interval appears to have been characterized not only by numerous CIEs, but
854 also a major switch in the timing and magnitude of these perturbations. Furthermore, there
855 was a rapid shoaling of carbonate dissolution horizons in the middle of the EECO. A key
856 finding of our study is that the major switch in planktic foraminiferal assemblages happened
857 at the start of the EECO. Significant, though ephemeral, modifications in planktic
858 foraminiferal assemblages coincide with numerous short-term CIEs, before, during and after
859 the EECO. Often, there are marked increases in the relative abundance of acarininids, similar
860 to what happened permanently across the start of the EECO.
861 Although we show for the first time that the critical turnover in planktic foraminifera
862 clearly coincided with the start of the EECO, the exact cause for the switch (aka the demise
863 of morozovellids) remains elusive. Possible causes are multiple, and may include temperature
864 effects on photosymbiont-bearing planktic foraminifera, changes in ocean chemistry, or even
865 interaction with other microplankton groups such as radiolarians, diatoms or dinoflagellates
866 that represented possible competitors in the use of symbionts or as symbiont providers. For
867 some reason, a critical threshold was surpassed at the start the EECO, and this induced an
868 unfavourable habitat for continued morozovellid diversification and proliferation but a

869 favourable habitat for the acarinids.

870

871 *Acknowledgements.* Funding for this research was provided by MIUR/PRIN COFIN 2010-
872 2011, coordinated by D. Rio. V. Luciani was financially supported by FAR from Ferrara
873 University, and L. Giusberti and E. Fornaciari received financial support from Padova
874 University (Progetto di Ateneo GIUSPRAT10). J. Backman acknowledges support from the
875 Swedish Research Council. We are grateful to Domenico Rio who promoted the researches
876 on the "Paleogene Veneto" and for the fruitful discussion. Members of the "Possagno net",
877 Simone Galeotti, Dennis Kent, Giovanni Muttoni, who sampled the section in 2003, are
878 gratefully acknowledged**.** We warmly acknowledge the Cementi Rossi s.p.a. and Mr. Silvano
879 Da Roit for fruitful collaboration during samplings at the Carcoselle Quarry (Possagno, TV).
880 This research used samples and data provided by the Ocean Drilling Program (ODP). ODP is
881 sponsored by the U.S. National Science Foundation (NSF) and participating countries under
882 management of Joint Oceanographic Institution (JOI) Inc. We specially thank from the ODP
883 Bremen Core Repository. Finally, we are grateful to the reviewers, B.Wade and R. Speijer,
884 who helped to strengthen the manuscript.

885

886 **References**

887

888 Abels, H. A., Clyde, W. C., Gingerich, P. D., Hilgen, F. J., Fricke, H. C., Bowen, G. J., and
889 Lourens, L. J.: Terrestrial carbon isotope excursions and biotic change during Palaeogene
890 hyperthermals, Nat. Geosci., 5, 326-329, doi: 10.1038/ngeo1427, 2012.
891 Agnini, C., Muttoni, G., Kent, D. V., and Rio, D.: Eocene biostratigraphy and magnetic
892 stratigraphy from Possagno, Italy: the calcareous nannofossils response to climate
893 variability, Earth Planet. Sci. Lett., 241, 815-830, 2006.

894 Agnini, C., Macrì, P., Backman, J., Brinkhuis, H., Fornaciari, E., Giusberti, L., Luciani, V.,
895 Rio, D., Sluijs, A., and Speranza, F.: An early Eocene carbon cycle perturbation at 52.5
896 Ma in the Southern Alps: chronology and biotic response, Paleoceanography, 24,
897 PA2209. doi: 10.1029/2008PA001649, 2009.
898 Agnini, C., Fornaciari, E., Giusberti, L., Grandesso, P., Lanci, L., Luciani, V., Muttoni, G.,
899 Plike, H., Rio, D., Spofforth, D.J.A., and Stefani, C.: Integrated biomagnetostratigraphy
900 of the Alano section (NE Italy): a proposal for defining the middle-late Eocene boundary,
901 Geol. Soc. Am. Bull., 123, 841-872, 2011.
902 Agnini, C., Spofforth, D. J. A., Dickens**,** G. R., Rio, D., Pälike, H., Backman, J., Muttoni, G.,
903 and Dallanave, E.: Stable isotope and calcareous nannofossil assemblage records for the
904 Cicogna section: toward a detailed template of late Paleocene and early Eocene global
905 carbon cycle and nannoplankton evolution, Clim. Past, under review, Special issue
906 Climatic and biotic events of the Paleogene, G. R. Dickens, V. Luciani, and A. Sluijs,
907 (Eds.), 2015.
908 Anderson, T. F., and Cole, S. A.: The stable isotope geochemistry of marine coccoliths: a
909 preliminary comparison with planktonic foraminifera, J. Foram. Res., 5 (3), 188-192,
910 1975.
911 Arthur , M. A., Dean, W. E., Bottjer, D., and Schole, P. A.: Rhythmic bedding in Mesozoic-
912 Cenozoic pelagic carbonate sequences: the primary and diagenetic origin of
913 Milankovitch like cycles, in: Milankovitch and Climate, A. Berger, J. Imbrie, J. Hays, G.
914 Kucla, B. Satzman (eds.), 191-222, D. Reidel Publ. Company, Dordrecht, Holland,
915 1984.
916 Arenillas, I., Molina, E., and Schmitz, B.: Planktic foraminiferal and $\delta^{13}C$ isotopic changes
917 across the Paleocene/Eocene boundary at Possagno (Italy), Int. J. Earth Sc., 88, 352–
918 364, 1999.

Aze, T., Ezard, T. H. G., Purvis, A., Coxall, H. K., Stewart, D. R. M, Wade, B. S., and Pearson, P. N.: A phylogeny of Cenozoic macroperforate planktonic foraminifera from fossil data, Biol. Rev., 86, 900-927. 900 doi: 10.1111/j.1469-185X.2011.00178.x, 2011.

Backman, J.: Late Paleocene to middle Eocene calcareous nannofossil biochronology from the Shatsky Rise, Walvis Ridge and Italy, Palaeogeogr. Palaeoclimatol. Palaeoecol., 57 (1), 43-59, 1986.

Bé, A. W. H.: Biology of planktonic foraminifera, in: Foraminifera: notes for a short course, Broadhead T., Stud. Geol., 6, Univ. Knoxville, Tenn., 51-92, 1982.

Bé, A. W. H., John, W. M., and Stanley, M. H.: Progressive dissolution and ultrastructural breakdown of planktic foraminifera, Cushman Foundation for Foraminiferal Research Special Publication, 13, 27-55, 1975.

Bé, A. W. H., Spero, H. J., and Anderson O. R.: Effects of symbiont elimination and reinfection on the life processes of the planktonic foraminifer *Globigerinoides sacculifer,* Marine Biol. 70, 73-86, 1982.

Bemis, B. E., Spero, H. J., Bijma, J., and Lea, D. W.: Reevaluation of the oxygen isotopic composition of planktonic foraminifera: Experimental results and revised paleotemperature equations, Paleoceanography, 13 (2), 150-160, 1998.

Berger, W. H.: Foraminiferal ooze: Solution at depth, Science*,* 156: 383-385, 1967.

Berger, W. H.: Planktonic foraminifera - selective solution and lysocline, Marine Geol., 8(2), 111-138, 1970.

Berger, W. H., Bonneau, M.-C., and. Parker, F. L.: Foraminifera on the deep-sea floor: lysocline and dissolution rate, Oceanol. Acta, 5 (2), 249-258, 1982.

Berggren, W. A., and Norris, R. D.: Biostratigraphy, phylogeny and systematics of Paleocene trochospiral planktic foraminifera, Micropaleont., 43 (Suppl. 1), 1-116, 1997.

Berggren, W. A., and Pearson, P. N.: A revised tropical to subtropical Paleogene planktic

foraminiferal zonation: J. Foram. Res., v. 35, p. 279-298, 2005.

Berggren, W. A., Kent, D. V., Swisher, C. C. III, and Aubry, M-P.: A revised Cenozoic geochronology and chronostratigraphy, in: Berggren W. A, Kent D. V., Aubry M-P., Hardenbol J. (Eds.), Geochronology, time scales and global stratigraphic correlation. SEPM Special Publication 54, 129-212, 1995.

Bleil, U.: The magnetostratigraphy of northwest Pacific sediments, Deep Sea Drilling Project Leg 86, Initial Reports Deep Sea Drilling Project, 86, 441-458.

Boersma, A., and Premoli Silva, I.: Paleocene planktonic foraminiferal biogeography and the paleoceanography of the Atlantic-Ocean, Micropaleont., 29, 355-381, 1983.

Boersma, A., Premoli Silva, I., and Shackleton, N.: Atlantic Eocene planktonic foraminiferal biogeography and stable isotopic paleoceanography, Paleoceanography, 2, 287-331, 1987.

Bohaty, S. M., and J. C. Zachos: A significant Southern Ocean warming event in the late middle Eocene, Geology, 31, 1017–1020, doi:10.1130/G19800.1, 2003.

Bohaty, S. M., Zachos, J. C., Florindo, F., and Delaney, M. L.: Coupled greenhouse warming and deep-sea acidification in the middle Eocene, Paleoceanography, 24, PA2207, doi:10.1029/2008PA001676, 2009.

Bolli, H. M.: Monografia micropaleontologica sul Paleocene e sull'Eocene di Possagno, Provincia di Treviso, Italia. Mémoires Suisses de Paléontologie 97: 222 pp., 1975.

Borre, M. and Fabricus, I.L.: Chemical and mechanical processes during burial diagenesis of chalk: an interpretation based on specific surface data of deep-sea sediments, Sedimentology, 45, 755-769, 1998.

Bosellini, A.: Dynamics of Tethyan carbonate platform, in: Controls on Carbonate Platform and Basin Platform, Crevello, P.D., Wilson, J.L., Sarg, J.F., Read, J.F., (Eds.), SEPM Spec. Publ., 44, 3-13, 1989.

969 Bowen, G. J., Bralower, T. J., Delaney, M. R., Dickens, G. R., Kelly, D. C., Koch, P. L.,
970 Kump, L. R., Meng, J., Sloan, L. C., Thomas, E., Wing, S. L., and Zachos, J. C.: Eocene
971 Hyperthermal Event Offers Insight Into Greenhouse Warming, EOS, 87 (17), 165-169,
972 DOI: 10.1029/2006EO170002, 2006.
973 Braga G.: L'assetto tettonico dei dintorni di Possagno (Trevigiano occidentale). Rendiconti
974 dell'Accademia Nazionale dei Lincei, 8/48: 451-455, 1970.
975 Bramlette, M. N., and Riedel, W. R.: Stratigraphic value of discoasters and some other
976 microfossils related to recent coccolithophores, J. Paleont., 28: 385-403, 1954.
977 Broecker, W. S., Clark, E., McCorkle D. C., Peng, T-H., Hajadas, I., and Bonani, G.:
978 Evidence of a reduction in the carbonate ion content of the deep see during the course of
979 the Holocene, Paleoceanography, 14 (6), 744-752, 1999.
980 Brown, J. H., Gillooly, J. F., Allen, A. P., Savage, V. M., and West, G. B.: Toward a
981 metabolic theory of ecology, Ecology, 85(7), 1771-1789, 2004.
982 Cita, M. B.: Stratigrafia della Sezione di Possagno, in: Bolli, H. M. (Ed.), Monografia
983 Micropaleontologica sul Paleocene e l'Eocene di Possagno, Provincia di Treviso, Italia,
984 Schweiz. Palaeontol. Abhandl., 97, 9–33, 1975.
985 Clyde, W. C., Gingerich, P. D., Wing, S. L., Röhl, U., Westerhold, T., Bowen, G., Johnson,
986 K., Baczynski, A. A., Diefendorf, A., McInerney, F., Schnurrenberger, D., Noren, A.,
987 Brady, K., and the BBCP Science Team: Bighorn Basin Coring Project (BBCP): A
988 continental perspective on early Paleogene hyperthermals, Scientific Drilling, 16, 21-31,
989 2013.
990 Coccioni, R., Bancalà, G., Catanzariti, R., Fornaciari, E., Frontalini, F., Giusberti, L., Jovane,
991 L., Luciani, V., Savian, J., and Sprovieri, M.: An integrated stratigraphic record of the
992 Palaeocene–lower Eocene at Gubbio (Italy): new insights into the early Palaeogene
993 hyperthermals and carbon isotope excursions, Terra Nova, 24, 380-386, 2012.

994 Coxall, H. K., Huber, B. T., and Pearson, P. N.: Origin and morphology of the Eocene
995 planktic foraminifera *Hantkenina,* J. Foram. Res., 33, 237-261, 2003.
996 Cramer, B. S., Wright, J. D., Kent, D. V., and Aubry, M.-P.: Orbital climate forcing of $\delta^{13}C$
997 excursions in the late Paleocene–early Eocene (chrons C24n–C25n), Paleoceanography,
998 18, 21-1. doi:10.1029/2003PA000909, 2003.
999 Cramer, B. S., Toggweiler, J. R., Wright, M. E., Katz, J. D., and Miller, K. G.: Ocean
1000 overturning since the Late Cretaceous: Inferences from a new benthic foraminiferal
1001 isotope compilation, Paleoceanography, 24, PA4216, doi:10.1029/2008PA001683, 2009.
1002 Crouch, E. M., Heilmann-Clausen, C., Brinkhuis, H., Morgans, H. E. G, Rogers, K.
1003 M., Egger, H., and Schmitz, B.: Global dinoflagellate event associated with the late
1004 Paleocene thermal maximum, Geology, 29(4), 315-318, 2001.
1005 D'Onofrio, R., Luciani V., Giusberti L., Fornaciari E., and Sprovieri, M.: Tethyan planktic
1006 foraminiferal record of the early Eocene hyperthermal events ETM2, H2 and I1 (Terche
1007 section, northeastern Italy), Rendiconti Online della Società Geologica Italiana, 31, 66-
1008 67, doi: 10.3301/ROL.2014.48, 2014.
1009 Dallanave, E., Agnini, C., Bachtadse, V., Muttoni, G., Crampton J. S., Strong, C. P., Hines,
1010 B. H., Hollis, C. J., and Slotnick, B. S.: Early to middle Eocene magneto-biochronology
1011 of the southwest Pacific Ocean and climate influence on sedimentation: Insights from the
1012 Mead Stream section, New Zealand, Geol. Soc. Am. Bull., 127 (5-6), 643-660, 2015.
1013 DeConto, R. M., Galeotti, S., Pagani, M., Tracy, D., Schaefer, K., Zhang, T., Pollard, D., and
1014 Beerling, D. J.: Past extreme warming events linked to massive carbon re-lease from
1015 thawing permafrost, Nature, 484, 87-92, http://dx.doi.org/10.1038/nature10929, 2012.
1016 Demicco, R. V.: Modeling seafloor-spreading rates through time, Geology, 32, 485-488,
1017 2004.
1018 Dickens, G. R.: Methane oxidation during the Late Palaeocene Thermal Maximum, B. Soc.

1019 Geol. Fr., 171 (1), 37-49, 2000.
1020 Dickens, G. R.: Down the Rabbit Hole: toward appropriate discussion of methane release
1021 from gas hydrate systems during the Paleocene–Eocene thermal maximum and other past
1022 hyperthermal events. Clim. Past, 7, 831-846. http://dx.doi.org/10.5194/cp-7-831-2011,
1023 2011.
1024 Dickens, G. R., and Backman J.: Core alignment and composite depth scale for the lower
1025 Paleogene through uppermost Cretaceous interval at Deep Sea Drilling Project Site 577,
1026 Newsl. Stratigr., 46, 47-68, 2013.
1027 Dickens, G. R., O'Neil, J. R., Rea, D. K., and Owen, R. M.: Dissociation of oceanic methane
1028 hydrate as a cause of the carbon isotope excursion at the end of the Paleocene,
1029 Paleoceanography, 10, 965-971, doi:10.1029/95PA02087, 1995.
1030 Dickens, G. R., Castillo, M. M., and Walker, J. C. G.: A blast of gas in the latest Paleocene:
1031 simulating first-order effects of massive dissociation of oceanic methane hydrate,
1032 Geology, 25, 259-262, 1997.
1033 Dunkley Jones, T., Lunt, D. J., Schmidt, D. N., Ridgwell, A., Sluijs, A., Valdez, P. J., and
1034 Maslin, M. A.: Climate model and proxy data constraints on ocean warming across the
1035 Paleocene–Eocene Thermal Maximum, Earth Sci. Rev., 125, 123-145, 2013.
1036 Edgar, K. M., Bohaty, S. M., Gibbs, S. J., Sexton, P. F., Norris, R. D., and Wilson, P. A.:
1037 Symbiont 'bleaching' in planktic foraminifera during the Middle Eocene Climatic
1038 Optimum, Geology, 41, 15-18, doi:10.1130/G33388.1, 2012.
1039 Falkowski, P. G., Katz, M. E., Milligan, A. J., Fennel, K., Cramer, B. S., Aubry, M. P.,
1040 Berner, R. A., Novacek, M. J., Zapol, W. M.: Mammals evolved, radiated, and grew in
1041 size as the concentration of oxygen in Earth's atmosphere increased during the past 100
1042 million years, Science, 309 (5744), 2202-2204, 2005.
1043 Figueirido, B., Janis, C. M., Pérez-Claros, J. A., De Renzi, M., and Palmqvist, P.: Cenozoic

climate change influences mammalian evolutionary dynamics, Proc. Natl. Acad. Sci. USA, 109 (3), 722-727, 2012.

Fletcher, B. J., Brentnall, S. J., Anderson, C. W., Berner, R. A., and Beerling, D.J.: Atmospheric carbon dioxide linked with Mesozoic and early Cenozoic climate change, Nature Geoscience, 1, 43-48, 2008.

Fornaciari, E., Giusberti, L., Luciani, V., Tateo, F., Agnini, C., Backman, J., Oddone, M., and Rio, D.: An expanded Cretaceous–Tertiary transition in a pelagic setting of the Southern Alps (central–western Tethys), Palaeogeogr. Palaeoclimatol. Palaeoecol., 255, 98-131, 2007.

Fraass, A. J., Kelly, D. K., and. Peters, S. E.: Macroevolutionary history of the planktic foraminifera, Annual Review of Earth and Planetary Sciences, 43, 139-66, doi: 10.1146/annurev-earth-060614-105059, 2015.

Frank, T. D., Arthur, M. A., and Dean, W. E.: Diagenesis of Lower Cretaceous pelagic carbonates, North Atlantic: paleoceanographic signals obscured, J. Foramin. Res., 29, 340-351, 1999.

Galeotti, S., Krishnan, S., Pagani, M., Lanci, L., Gaudio, A., Zachos, J. C., Monechi, S., Morelli, G., and Lourens, L. J.: Orbital chronology of early Eocene hyperthermals from the Contessa Road section, central Italy, Earth Planet. Sci. Lett., 290(1-2), 192-200, doi: 10.1016/j.epsl.2009.12.021, 2010.

Gingerich, P. D.: Rates of evolution on the time scale of the evolutionary process, Genetica, 112-113, 127-144, 2001.

Gingerich, P. D.: Mammalian response to climate change at the Paleocene–Eocene boundary: Polecat Bench record in the northern Bighorn Basin, Wyoming, Geol. Soc. Am. Spec. Pap., 369, 463-478, 2003.

Giusberti, L., Rio, D., Agnini, C., Backman, J., Fornaciari, E., Tateo, E., and Oddone, M.:

1069 Mode and tempo of the Paleocene–Eocene thermal maximum in an expanded section
1070 from the Venetian pre-Alps, Geol. Soc. Am. Bull., 119, 391-412, 2007.
1071 Hallock, P.: Fluctuations in the trophic resource continuum: a factor in global diversity
1072 cycles? Paleoceanography, 2, 457–471, 1987.
1073 Hancock, H. J. L., and Dickens, G. R.: Carbonate dissolution episodes in Paleocene and
1074 Eocene sediment, Shatsky Rise, west-central Pacific, Proc. Ocean Drill. Progr., Sci.
1075 Results 198, 24 pp., doi:10.2973/odp.proc.sr.198.116., 2005.
1076 Hemleben, C, Spindler, M., and Anderson, O. R (Eds.).: Modern planktonic foraminifera,
1077 Springer-Verlag, New York, 1-363, ISBN-13: 9780387968155, 1989.
1078 Hilgen, F. J., Abels, H. A., Kuiper, K. F., Lourens, L. J., and Wolthers, M.: Towards a stable
1079 astronomical time scale for the Paleocene: aligning Shatsky Rise with the Zumaia –
1080 Walvis Ridge ODP Site 1262 composite, Newsl. Stratigr., 48, 91-110, doi:
1081 10.1127/nos/2014/0054, 2015.
1082 Hollis, C. J., Taylor, K. W. R., Handley, L., Pancost, R. D., Huber, M., Creech, J. B., Hines,
1083 B. R., Crouch, E. M., Morgans, H. E. G., Crampton, J. S., Gibbs, S., Pearson, P. N., and
1084 Zachos, J. C.: Early Paleogene temperature history of the Southwest Pacific Ocean:
1085 Reconciling proxies and models: Earth Planet. Sci. Lett., 349-350, 53–66, doi:
1086 10.1016/j.epsl.2012.06.024, 2012.
1087 Huber, M., and Caballero, R.: The early Eocene equable climate problem revisited. Clim.
1088 Past, 7, 603-633, 2011.
1089 Hyland, E. G., and Sheldon, N. D.: Coupled CO2-climate response during the Early Eocene
1090 Climatic Optimum, Palaeogeogr. Palaeoclimatol. Palaeoecol., 369, 125-135, 2013.
1091 Hyland, E. G., Sheldon, N. D., and Fan, M.: Terrestrial paleoenvironmental reconstructions
1092 indicate transient peak warming during the early Eocene climatic optimum, Geol. Soc.
1093 Am. Bull., 125 (7-8), 1338-1348, 2013.

IPCC, 2014: Climate Change 2014: Synthesis Report. Contribution of Working Groups I, II and III to the Fifth Assessment Report of the Intergovernmental Panel on Climate Change [Core Writing Team, R.K. Pachauri and L.A. Meyer (eds.)]. IPCC, Geneva, Switzerland, 151 pp, 2014.

Inglis, G. N., Farnsworth, A., Lunt, D., Foster, G. L., Hollis, C. J., Pagani, M., Jardine, P. E., Pearson, P. N., Markwick, P., Galsworthy, A. M. J., Raynham, L., Taylor, K. W. R., and Pancost, R. D.: Descent toward the icehouse: Eocene sea surface cooling inferred from GDGT distributions. Paleoceanography, 30 (7), 100-1020, 10.1002/2014PA002723, 2015.

Ito, G., and Clift, P. D.: Subsidence and growth of Pacific Cretaceous plateaus. Earth Plant. Sci. Lett., 161, 85-100, 1998.

John E. H., Pearson P. N., Coxall H. K., Birch H., Wade B. S., and Foster G. L.: Warm ocean processes and carbon cycling in the Eocene, Phil. Trans. R. Soc., A, 371, 20130099, 2013.

John E. H., Wilson J. D., Pearson P. N., and Ridgwell, A.: Temperature-dependent remineralization and carbon cycling in the warm Eocene oceans, Palaeogeogr. Palaeoclimatol. Palaeoecol., 413, 158-166, 2014.

Kelly, D. C., Bralower, T. J., Zachos, J. C., Premoli Silva, I., and Thomas, E.: Rapid diversification of planktonic foraminifera in the tropical Pacific (ODP Site 865) during the late Paleocene thermal maximum, Geology 24, 423-426, 1996.

Kelly, D. C., Bralower, T. J., and Zachos, J. C.: Evolutionary consequences of the latest Paleocene thermal maximum for tropical planktonic foraminifera, Palaeogeogr., Palaeoclimatol., Palaeoecol., 141, 139-161, 1998.

Kennett, J. P., and Stott, L. D.: Abrupt deep-sea warming, palaeoceanographic changes and benthic extinctions at the end of the Palaeocene, Nature 353, 225-229, 1991.

1119 Kirtland-Turner, S., Sexton P. F., Charled C. D., and Norris R. D.: Persistence of carbon
1120 release events through the peak of early Eocene global warmth, Nature Geoscience, 7,
1121 748-751, doi: 10.1038/NGEO2240, 2014.
1122 Komar, N., Zeebe, R. E., and Dickens, G. R.: Understanding long-term carbon cycle trends:
1123 the late Paleocene through the early Eocene, Paleoceanography, 28, 650-662, doi:
1124 10.1002/palo.20060, 2013.
1125 Kroenke, L. W., Berger, W. H., Janecek, T. R., et al.: Ontong Java Plateau, Leg 130: synopsis
1126 of major drilling results, Proceedings of the Ocean Drilling Program, Initial Reports, 130,
1127 497-537, 1991.
1128 Kurtz, A. C., Kump, L. R., Arthur, M. A., Zachos, J. C., and Paytan, A.: Early Cenozoic
1129 decoupling of the global carbon and sulfur cycles, Paleoceanography, 18, 1090, doi:
1130 10.1029/2003PA000908, 2003.
1131 Lauretano, V., Littler, K., Polling, M., Zachos, J. C., and Lourens, L. J.: Frequency,
1132 magnitude and character of hyperthermal events at the onset of the Early Eocene
1133 Climatic Optimum, Clim. Past, 11, 1313-1324, doi: 10.5194/cp-11-1313-2015, 2015.
1134 Lee C. T., Shen B., Slotnick B. S., Liao K., Dickens G. R., Yokoyama Y., Lenardic A.,
1135 Dasgupta R., Jellinek M., Lackey J. S., Schneider T., and Tice M. M.: Continental arc-
1136 island arc fluctuations, growth of crustal carbonates, and long-term climate change,
1137 Geosphere, 9, 21-36, 2013.
1138 LeGrande, A. N. and Schmidt, G. A.: Global gridded data set of the oxygen isotopic
1139 composition in seawater, Geophys. Res. Lett., 33, L12604, doi: 10.1029/2006GL026011,
1140 2006.
1141 Leon-Rodriguez, L. and Dickens, G. R.: Constraints on ocean acidification associated with
1142 rapid and massive carbon injections: The early Paleogene record at ocean drilling
1143 program site 1215, equatorial Pacific Ocean, Palaeogeogr. Palaeoclimatol. Palaeoecol.,

298 (3-4), 409-420, doi: 10.1016/j.palaeo.2010.10.029, 2010.

Lirer, F.: A new technique for retrieving calcareous microfossils from lithified lime deposits. Micropaleontol., 46, 365–369, 2000.

Littler, K., Röhl, U., Westerhold, T., and Zachos, J. C.: A high-resolution benthic stable-isotope for the South Atlantic: implications for orbital-scale changes in Late Paleocene-early Eocene climate and carbon cycling, Earth Planet. Sci. Lett., 401, 18-30. http://dx.doi.org/10.1016/j.epsl.2014.05.054, 2014.

Lourens, L. J., Sluijs, A., Kroon, D., Zachos, J. C., Thomas, E., Röhl, U., Bowles, J., and Raffi, I.: Astronomical pacing of late Palaeocene to early Eocene global warming events, Nature, 7045, 1083-1087, 2005.

Lowestein, T. K., and Demicco R. V.: Elevated Eocene atmospheric CO_2 and its subsequent decline, Science, 313 (5795), doi: 10.1126/science.1129555, 2006.

Lu, G.: Paleocene-Eocene transitional events in the ocean: Faunal and isotopic analyses of planktic foraminifera, Ph.D. Thesis, Princeton University, pp. 1-284, 1995.

Lu, G., and Keller, G.: Planktic foraminiferal faunal turnovers in the subtropical Pacific during the late Paleocene to early Eocene, J. Foramin. Res., 25 (2), 97-116, 1995.

Lu, G., Keller, G. and Pardo, A.: Stability and change in Tethyan planktic foraminifera across the Paleocene-Eocene transition, Mar. Micropaleont., 35 (3-4), 203-233, 1998.

Luciani, V., Giusberti, L., Agnini, C., Backman, J., Fornaciari, E., and Rio., D.: The Paleocene–Eocene Thermal Maximum as recorded by Tethyan planktonic foraminifera in the Forada section (northern Italy), Mar. Micropaleont., 64, 189-214, 2007.

Luciani, V., Giusberti, L., Agnini, C., Fornaciari, E., Rio, D., Spofforth, D. J. A., and Pälike H.: Ecological and evolutionary response of Tethyan planktonic foraminifera to the middle Eocene climatic optimum (MECO) from the Alano section (NE Italy), Palaeogeogr. Palaeoclimatol. Palaeoecol., 292, 82-95, doi: 10.1016/j.palaeo.2010.03.029,

2010.

Luciani, V., and Giusberti, L.: Reassessment of the early–middle Eocene planktic foraminiferal biomagnetochronology: new evidence from the Tethyan Possagno section (NE Italy) and Western North Atlantic Ocean ODP Site 1051, J. Foram. Res., 44, 2, 187-201, 2014.

Lunt, D. J., Ridgwell, A., Sluijs, A., Zachos, J., Hunter, S., and Haywood, A.: A model for orbital pacing of methane hydrate destabilization during the Palaeogene, Nat. Geosc., 4, 775-778, doi: 10.1038/NGEO1266, 2011.

Marshall, J. D.: Climatic and oceanographic isotopic signals from the carbonate rock records and their preservation, Geol. Mag., 129, 143-160, 1992.

Matter, A., Douglas, R. G., and Perch-Nielsen, K: Fossil preservation, geochemistry and diagenesis of pelagic carbonates from Shatsky Rise, northwest Pacific, Initial Reports Deep Sea Drilling Project, 32, 891-922, doi: 10.2973/dsdp.proc.32.137, 1975.

McInerney, F. A. and Wing, S. L.: The Paleocene–Eocene thermal maximum: a perturbation of carbon cycle, climate, and biosphere with implications for the future, Ann. Rev. Earth Planet. Sci., 39, 489-516, doi: 10.1146/annurev-earth-040610-133431, 2011.

Mita, I.: Data Report: Early to late Eocene calcareous nannofossil assemblages of Sites 1051 and 1052, Blake Nose, Northwestern Atlantic Ocean, Proc. Ocean Drilling Program, Sci. Results, 171B, 1-28, 2001.

Molina, E., Arenillas, I., Pardo, A.: High resolution planktic foraminiferal biostratigraphy and correlation across the Palaeocene Palaeocene/Eocene boundary in the Tethys, B. Soc. Géol. Fr., 170, 521–530, 1999.

Monechi, L., Bleil, U., and Backman, J.: Magnetobiochronology of Late Cretaceous-Paleogene and late Cenozoic pelagic sedimentary sequences from the northwest Pacific (Deep Sea Drilling Project, Leg 86, Site 577. Proceedings of the Ocean Drilling Program

86, Initial Reports, Ocean Drilling Program, College Station, TX, doi:10.2973/dsdp.proc.86.137.1985.

Nguyen, T. M. P., Petrizzo, M.-R., and Speijer, R. P.: Experimental dissolution of a fossil foraminiferal assemblage (Paleocene–Eocene Thermal Maximum, Dababiya, Egypt): implications for paleoenvironmental reconstructions, Mar. Micropaleontol., 73 (3-4), 241-258, doi: 10.1016/j.marmicro.2009.10.005, 2009.

Nguyen, T. M. P., Petrizzo, M.-R., Stassen, P., and Speijer, R. P.: Dissolution susceptibility of Paleocene–Eocene planktic foraminifera: Implications for palaeoceanographic reconstructions, Mar. Micropaleont., 81, 1-21, 2011.

Nicolo, M. J., Dickens, G. R., Hollis, C. J., and Zachos, J. C.: Multiple early Eocene hyperthermals: their sedimentary expression on the New Zealand continental margin and in the deep sea, Geology, 35, 699-702, 2007.

Norris, R.D.: Biased extinction and evolutionary trends, Paleobiology, 17 (4), 388-399, 1991.

Norris, R.: Symbiosis as an evolutionary innovation in the radiation of Paleocene planktic foraminifera, Paleobiology, 22, 461-480, 1996.

Norris, R. D., Kroon, D., and Klaus, A.: Proceedings of the Ocean Drilling Program, Initial Reports, 171B, Proc. Ocean Drill. Progr. Sci. Results, 1-749, 1998.

O'Connor, M., Piehler, M. F., Leech, D. M., Anton, A., and Bruno, J. F.: Warming and resource availability shift food web structure and metabolism, PLOS Biol., 7(8), 1-6. doi: 10.1371/journal.pbio.1000178, 2009.

Ogg, J. G., and Bardot, L.: Aptian through Eocene magnetostratigraphic correlation of the Blake Nose Transect (Leg 171B), Florida continental margin, Proc. Ocean Drill. Progr., Sci. Results, 171B, 1-58, doi: 10.2973/odp.proc.sr.171B.104.2001

Olivarez Lyle, A., and Lyle, M. W.: Missing organic carbon in Eocene marine sediments: Is metabolism the biological feedback that maintains end-member climates?

1219 Paleoceanography, 21, PA2007, doi: 10.1029/2005PA001230, 2006.
1220 Oreshkina, T. V.: Evidence of late Paleocene - early Eocene hyperthermal events in
1221 biosiliceous sediments of Western Siberia and adjacent areas, Austrian Journal of Earth
1222 Science, 105, 145-153, 2012.
1223 Pälike, H., Lyle, M. W., Nishi, H., Raffi, I., Ridgwell, A., Gamage, K., Klaus, A., Acton, G.,
1224 Anderson, L., Backman, J., Baldauf, J., Beltran, C., Bohaty S. M., Bown, P., Busch, W.
1225 Channell, J. E. T., Chun, C. O. J., Delaney, M., Dewangan, P., Dunkley Jones, T., Edgar,
1226 K. M., Evans, H., Fitch, P. L., Foster, G. L., Gussone, N., Hasegawa, H., Hathorne, E. C.,
1227 Hayashi, H., Herrle, J. O., Holbourn, A., Hovan, S., Hyeong, K., Iijima, K., Ito, T.,
1228 Kamikuri, S., Kimoto, K., Kuroda, J., Leon-Rodriguez, L., Malinverno, A., Moore, T. C.,
1229 Brandon, H., Murphy, D. P., Nakamura, H., Ogane, K., Ohneiser, C. Richter, C.,
1230 Robinson, R., Rohling, E. J., Romero, O., Sawada, K., Scher, H., Schneider, L., Sluijs,
1231 A., Takata, H., Tian, J., Tsujimoto, A., Wade, B. S., Westerhold, T., Wilkens, R.,
1232 Williams, T., Wilson, P. A., Yamamoto, Y., Yamamoto, S., Yamazaki, T., and Zeebe, R.
1233 E.: Cenozoic record of the equatorial Pacific carbonate compensation depth, Nature, 488,
1234 609-614, doi: 10.1038/nature11360, 2012, 2012.
1235 Pearson P.N., Coxall H.K.: Origin of the Eocene planktonic foraminifer *Hantkenina* by
1236 gradual evolution, Palaeontology, 57, 243-267, 2014.
1237 Pearson, P. N., and Palmer, M. R.: Atmospheric carbon dioxide concentrations over the past
1238 60 million years, Nature, 406, 695-699, doi: 10.1038/35021000, 2000.
1239 Pearson, P.N., Shackleton, N.J., Hall, M.A.: Stable isotope paleoecology of middle Eocene
1240 planttonic foraminifera and multi-species isotope stratigraphy, DSDP Site 523, south
1241 Atlantic, J. Foram. Res. 23, 123-140, 1993.
1242 Pearson, P.N., Ditchfield, P.W, Singano, J., Harcourt-Brown, K.G., Nicholas, C.J., Olsson,
1243 R.K, Shackleton, N.J., Hall, M.A.: Warm tropical sea surface temperatures in the Late

1244 Cretaceous and Eocene epochs, Nature, 413, 481-487, 2001. doi:10.1038/35097000,
1245 2001.
1246 Pearson, P. N., Olsson, R. K., Huber, B. T., Hemleben, C., and Berggren, W.A. (Eds.): Atlas
1247 of Eocene planktonic foraminifera, Cushman Found. Foram. Res., Spec. Publ. 41, 1-514,
1248 2006.
1249 Petrizzo, M.R.: The onset of the Paleocene–Eocene Thermal Maximum (PETM) at Sites
1250 1209 and 1210 (Shatsky Rise, Pacific Ocean) as recorded by planktonic foraminifera,
1251 Mar. Micropaleont., 63, 187–200, 2007.
1252 Petrizzo, M.-R., Leoni, G., Speijer, R. P., De Bernardi, B., and Felletti, F.: Dissolution
1253 susceptibility of some Paleogene planktonic foraminifera from ODP Site 1209 (Shatsky
1254 Rise, Pacific Ocean), J. Foram. Res. 38, 357-371, 2008.
1255 Pross, J., Contreras, L., Bijl, P. K., Greenwood, D. R., Bohaty, S. M., Schouten, S., Bendle J.
1256 A., Röhl, U., Tauxe, L., Raine, J. I., Claire E., Huck, C. E., van de Flierdt, T., Stewart S.
1257 R. Jamieson, S. S. R., Stickley, C. E., van de Schootbrugge, B., Escutia, C., and
1258 Brinkhuis, H.: Persistent near-tropical warmth on the Antarctic continent during the early
1259 Eocene Epoch: Nature, v. 488, 73-77, doi: 10 .1038 /nature11300, 2012.
1260 Pujalte, V., Baceta, J. G., and Schmitz, B.: A massive input of coarse-grained siliciclastics in
1261 the Pyrenean Basin during the PETM: the missing ingredient of a coeval abrupt change
1262 in hydrological regime, Clim. Past, under review, Special issue Climatic and biotic
1263 events of the Paleogene, G. R. Dickens, V. Luciani, and A. Sluijs, (Eds.), 2015.
1264 Quillévéré, F., Norris, R. D., Moussa, I., and Berggren, W. A.: Role of photosymbiosis and
1265 biogeography in the diversification of early Paleogene acarininids (planktonic
1266 foraminifera), Paleobiology, 27, 311-326, 2001.
1267 Raymo, M. E., and Ruddiman W. F.: Tectonic forcing of late Cenozoic climate, Nature, 359,
1268 117-122, 1992.

1269 Reghellin, D., Coxall, H. K., Dickens, G. R., and Backman, J.: Carbon and oxygen isotopes
1270 of bulk carbonate in sediment deposited beneath the eastern equatorial Pacific over the
1271 last 8 million years. Paleoceanography, 30: 1261-1286. doi: 10.1002/2015PA002825,
1272 2015.
1273 Röhl, U., Westerhold, T., Monechi, S., Thomas, E., Zachos, J. C., and Donner, B.: The third
1274 and final early Eocene Thermal Maximum: characteristics, timing, and mechanisms of
1275 the "X" event, Geol. Soc. Am. Abstracts with Program, 37(7), 264, 2005.
1276 Schlanger, S.O. and Douglas, R.G.: The pelagic ooze-chalk-limestone transition and its
1277 implications for marine stratigraphy, In: Pelagic Sediments: on Land and under the Sea,
1278 K.J. Hsü and H.C. Jenkyns (Eds.), Spec. Publs. Ass. Sediment., 1, 117–148, 1974.
1279 Scholle, P. A., and Arthur, M. A.: Carbon isotope fluctuations in Cretaceous pelagic
1280 limestones: potential stratigraphic and petroleum exploration tool, American Association
1281 of Petroleum Geologists Bulletin, 64, 67-87, 1980.
1282 Schmitz, B., and Puljate, V.: Abrupt increase in seasonal extreme precipitation at the
1283 Paleocene-Eocene boundary, Geology, 35, 215-218, 2007.
1284 Schmidt, D. N., Thierstein, H. R., and Bollmann, J.: The evolutionary history of size variation
1285 of planktic foraminiferal assemblages in the Cenozoic, Palaeogeogr. Palaeoclimatol.
1286 Palaeoecol., 212, 159-180, doi: 10.1016/j.palaeo.2004.06.002, 2004.
1287 Schneider, L. J. Bralower, T. J., and Kump, L. J.: Response of nannoplankton to early Eocene
1288 ocean destratification, Palaeogeogr. Palaeoclimatol. Palaeoecol., 310, 152-162, 2011.
1289 Schrag, D. P., DePaolo, D. J., and Richter, F. M.: Reconstructing past sea surface
1290 temperatures: correcting for diagenesis of bulk marine carbonate, Geochim. Cosmochim.
1291 Ac., 59, 2265-2278, 1995.
1292 Sexton, P.F., Wilson, P.A., Norris, R.D.: Testing the Cenozoic multisite composite $\delta^{18}O$ and
1293 $\delta^{13}C$ curves: New monospecific Eocene records from a single locality, Demerara Rise

(Ocean Drilling Program Leg 207), Paleoceanography, 21, PA2019, 2006.

Sexton, P. F., Norris R. D., Wilson, P. A., Pälike, H., Westerhold, T., Röhl, U., Bolton, C. T., and Gibbs, S.: Eocene global warming events driven by ventilation of oceanic dissolved organic carbon, Nature 471, 349-353, doi: 10.1038/nature09826, 2011.

Shackleton, N. J.: Paleogene stable isotope events. Palaeogeogr. Palaeoclim. Palaeoecol., 57, 91-102, 1986.

Shackleton, N. J., and Hall, M. A.: Stable isotope records in bulk sediments (Leg 138), Proc. Ocean Drill. Progr. Sci. Results, 138, 797-805, doi:10.2973/odp.proc.sr.138.150.1995.

Shamrock, J. L., Watkins, D. K., and Johnston, K. W.: Eocene bio-geochronology of ODP Leg 122 Hole 762C, Exmouth Plateau (northwest Australian Shelf), Stratigraphy, 9, 55-76, 2012.

Shipboard Scientific Party, 1985, Site 577: Initial Reports Deep Sea Drilling Project, 86, in: Heath, G.R., Burckle, L.H., et al. (Eds.), Washington (U.S. Government Printing Office), 91–137. doi:10.2973/dsdp.proc.86.104.1985, 1995.

Shipboard Scientific Party, 1998, Site 1051: Proceeding Ocean Drilling Program, Initial Reports, 171B, in: Norris, R.D., Kroon, D., Klaus, A., et al (Eds.), Ocean Drilling Program, College Station, TX, 171–239. doi:10.2973/odp.proc.ir.171b.105.1998, 1998.

Sims, P. A., Mann, D. G., and Medlin, L. K.: Evolution of the diatoms: insights from fossil, biological and molecular data, Phycologia, 45, 361-402, 2006.

Sinton, C. W., and Duncan R. A.: ^{40}Ar-^{39}Ar ages of lavas from the southeast Greenland margin, ODP Leg 152, and the Rockall Plateau, DSDP Leg 81, Ocean Drill. Progr., Sci. Res., 152, 387-402, doi:10.2973/odp.proc.sr.152.234.1998, 1998.

Slotnik, B. S., Dickens, G. R., Nicolo, M. J., Hollis, C. J., Crampton, J. S., Zachos, J. C., and Sluijs, A.: Large-amplitude variations in carbon cycling and terrestrial weathering during the latest Paleocene and earliest Eocene: The Record at Mead Stream, New Zealand, J.

1319 Geol., 120, 487-505, 2012.
1320 Slotnick, B. S., Dickens, G. R., Hollis, C. J., Crampton, J. S., Percy Strong, C., and Zachos, J.
1321 C.: Extending lithologic and stable carbon isotope records at Mead Stream (New
1322 Zealand) through the middle Eocene, in: Dickens G.R., Luciani V. eds. Climatic and
1323 biotic events of the Paleogene 2014 CBEP 2014 Volume 31, Roma, Società Geologica
1324 Italiana, 201-202, 2014.
1325 Slotnick, B. S., Dickens, G. R., Hollis, C. J., Crampton, J. S., Strong, P. S. and Phillips, A.:
1326 The onset of the Early Eocene Climatic Optimum at Branch Stream, Clarence River
1327 valley, New Zealand, New Zeal. J. Geol. Geop., doi: 10.1080/00288306.2015.1063514,
1328 2015a.
1329 Slotnick, B. S., Laurentano, V., Backman, J., Dickens, G. R., Sluijs, A., and Lourens, L.:
1330 Early Paleogene variations in the calcite compensation depth: new constraints using old
1331 borehole sediments from across Ninetyeast Ridge, central Indian Ocean, Clim. Past, 11,
1332 472-493, 2015b.
1333 Sluijs, A., and Dickens, G. R.: Assessing offsets between the $\delta^{13}C$ of sedimentary
1334 components and the global exogenic carbon pool across early Paleogene carbon cycle
1335 perturbations, Global Biogeochem. Cy., 26 (4), GB4019, doi: 10.1029/2011GB004094,
1336 2012.
1337 Sluijs, A., Schouten, S., Pagani, M., Woltering, M., Brinkhuis, H., Sinninghe Damsté, J. S.,
1338 Dickens, G. R., Huber, M., Reichart, G., Stein, R., Matthiessen, J., Lourens, L. J.,
1339 Pedentchouk, N., Backman, J., Moran, K., and the Expedition 302 Scientists: Subtropical
1340 Arctic Ocean temperatures during the Palaeocene/Eocene thermal maximum, Nature,
1341 441, 610-613, doi: 10.1038/nature04668, 2006.
1342 Sluijs, A., Bowen, G. J., Brinkhuis, H., Lourens, L. J., and Thomas, E.: The Paleocene–
1343 Eocene thermal maximum super greenhouse: biotic and geochemical signatures, age

models and mechanisms of global change, in: Deep-Time Perspectives on Climate Change, Williams, M., Haywood, A. M., Gregory, F. J., and Schmidt, D. N., (Eds.), Micropalaeont. Soc. Spec. Publ., Geological Society, London, 323-350, 2007.

Smith, R. Y., Greenwood, D. R., and Basinger, J. F.: Estimating paleoatmospheric pCO_2 during the Early Eocene Climatic Optimum from stomatal frequency of Ginkgo, Okanagan Highlands, British Columbia, Canada, Palaeogeogr. Palaeoclimatol. Palaeoecol., 293, 120-131, 2010.

Stap, L., Sluijs, A., Thomas, E., and Lourens L. J.: Patterns and magnitude of deep sea carbonate dissolution during Eocene Thermal Maximum 2 and H2, Walvis Ridge, southeastern Atlantic Ocean, Paleoceanography, 24, 1211, doi: 10.1029/2008PA001655, 2009.

Thomas, E.: Biogeography of the late Paleocene benthic foraminiferal extinction, in: Late Paleocene-early Eocene climatic and biotic events in the marine and terrestrial Records, Aubry, M.-P., Lucas, S., and Berggren, W. A., (Eds.), Columbia University Press, New York, 214-243, 1998.

Thomas, E., Brinkhuis, H., Huber, M., and Röhl**,** U.: An ocean view of the early Cenozoic Greenhouse world, Oceanography, 19, 94-103, 2006.

Thunell R. C. and Honjo, S.: Calcite dissolution and the modification of planktonic foraminiferal assemblages, Mar. Micropaleont., 6, 169-182, 1981.

Vandenberghe N., Hilgen F. J., Speijer R. P., Ogg J. G., Gradstein F. M., Hammer O., Hollis C. J., and Hooker J. J.: The Paleogene Period, in: Gradstein, F., Ogg, J.G., Schmitz, M.D., Ogg, G.M., (Eds.), The Geologic Time Scale 2012, 855-921, Elsevier, Amsterdam, 2012.

Vincent, E., and Berger, W. H: Planktonic foraminifera and their use in paleoccanography; in: Emiliani. C (Ed.), The Sea, 7 (25), New York, 1025-1119, 1981.

1369 Vogt, P. R.: Global magmatic episodes: New evidence and implications for the steady state
1370 mid-oceanic ridge, Geology, 7, 93-98, 1979.
1371 Wade, B. S.: Planktonic foraminiferal biostratigraphy and mechanisms in the extinction of
1372 *Morozovella* in the late Middle Eocene, Mar. Micropaleont., 51, 23–38, 2004.
1373 Wade, B. S., Al-Sabouni, N., Hemleben, C., and Kroon, D.: Symbiont bleaching in fossil
1374 planktonic foraminifera, Evol. Ecol., 22, 253-265. doi: 10.1007/s10682-007-9176-6,
1375 2008.
1376 Wade, B. S., Pearson, P. N., Berggren, and W. A., Pälike, H.: Review and revision of
1377 Cenozoic tropical planktonic foraminiferal biostratigraphy and calibration to the
1378 geomagnetic polarity and astronomical time scale, Earth Sci. Rev., 104, 111-142, doi:
1379 10.1016/j.earscirev.2010.09.003, 2011.
1380 Wade, B.S., Fucek, V.P., Kamikuri, S.-I., Bartol, M., Luciani, V., Pearson, P.N.: Successive
1381 extinctions of muricate planktonic foraminifera (*Morozovelloides* and *Acarinina*) as a
1382 candidate for marking the base Priabonian, Newsl. Stratigr., 45 (3) 245-262, 2012.
1383 Westerhold, T., Röhl**,** U., Frederichs, T., Bohaty, S. M., and Zachos, J. C.: Astronomical
1384 calibration of the geological timescale: closing the middle Eocene gap, Clim. Past, 11,
1385 1181–1195, doi: 10.5194/cp-11-1181-2015, 2015.
1386 Wilf, P., Cúneo, R. N., Johnson, K. R., Hicks, J. F., Wing, S. L., and Obradovich, J. D.: High
1387 plant diversity in Eocene South America: evidence from Patagonia, Science, 300, 122-
1388 125, 2003.
1389 Wing, S. L., Bown, T. M., and Obradovich, J. D.: Early Eocene biotic and climatic change in
1390 interior western North America, Geology 19, 1189-1192, 1991.
1391 Woodbourne, M. O., Gunnell, G. F., and Stucky, R. K.: Climate directly influences Eocene
1392 mammal faunal dynamics in North America, P. Natl. Acad. Sci. USA, 106 (32), 13399-
1393 13403, 2009.

1394 Yapp, C.J.: Fe(CO_3)OH in goethite from a mid-latitude North American Oxisol: Estimate of
1395 atmospheric CO_2 concentration in the early Eocene "climatic optimum". Geochim.
1396 Cosmochim. Ac., 68(5), 935-947. doi: 10.1016/j.gca.2003.09.002, 2004.
1397 Zachos, J. C., Pagani, M., Sloan, L., Thomas, E., and Billups, K.: Trends, rhythms, and
1398 aberrations in global climate 65 Ma to Present, Science, 292, 686-693, 2001.
1399 Zachos, J. C., Röhl, U., Schellenberg, S. A., Sluijs, A., Hodell, D. A., Kelly, D. C., Thomas,
1400 E., Nicolo, M., Raffi, I., Lourens, L. J., McCarren, H., and Kroon, D.: Rapid acidification
1401 of the ocean during the Paleocene–Eocene thermal maximum, Science, 308, 1611-161,
1402 2005.
1403 Zachos, J. C., Dickens, G. R., and Zeebe, R. E.: An early Cenozoic perspective on
1404 greenhouse warming and carbon-cycle dynamics, Nature, 451, 279-283, 2008.
1405 Zachos, J. C., McCarren, H., Murphy, B., Röhl, U., and Westerhold, T.: Tempo and scale of
1406 late Paleocene and early Eocene carbon isotope cycles: Implications for the origin of
1407 hyperthermals, Earth Planet. Sci. Lett., 299, 242-249, doi: 10.1016/j.epsl.2010.09.004,
1408 2010.
1409 Zeebe, R. E., Zachos, J. C., Dickens, G. R.: Carbon dioxide forcing alone insufficient to
1410 explain Palaeocene–Eocene Thermal Maximum warming. Nat. Geosci.2 (8), 576-580,
1411 http://dx.doi.org/10.1038/ngeo578, 2009.
1412 Zonneveld, J. P., Gunnell, G. F., and Bartels, W. S.: Early Eocene fossil vertebrates from the
1413 southwestern Green River Basin, Lincoln and Uinta Counties, Wyoming, Journal of
1414 Vertebrate Paleontology, 20, 369-386, 2000.
1415
1416
1417
1418

Figure Captions

Figure 1. The evolution of climate, carbon cycling, and planktic foraminifera across the middle Paleogene on the GPTS 2012 time scale. The left side of the figure shows polarity chrons, and smoothed oxygen and carbon isotope records of benthic foraminifera, slightly modified from Vandenberghe et al. (2012, Fig. 28.11). The original oxygen and carbon isotope values come from numerous sources as compiled by Zachos et al. (2008) and Cramer et al. (2009). The middle part of the figure indicates planktic foraminifer biozones as presented by Wade et al. (2011), and partly modified by Luciani and Giusberti (2014) who proposed a different definition of lower boundary of Zone E7a. This boundary is now based on the first occurrence of *Astrorotalia palmerae* due to diachronous first appearance of the previous selected marker *A. cuneicamerata*. In addition, the base of Zone E5, identified by the first appearance of *Morozovella aragonensis,* occurs within the mid C24n instead of lower C23r. We add a question mark at the *Morozovella subbotinae* top because the present study highlights a remarkable diachronism of this event (see text). The right side of the figure shows a partial view of morozovellids and acarininids evolution as suggested by Aze et al. (2011). It does not include several "root taxa" that disappear in the earliest Eocene (e.g., *M. velascoensis*) or "excursion taxa" that appear during the Paleocene-Eocene Thermal Maximum (PETM) (e.g., *M. allisonensis*). Superimposed on these records are key intervals of climate change, including the Early Eocene Climatic Optimum (EECO), the Middle Eocene Climatic Optimum (MECO) and the three well documented early Eocene hyperthermals. The shown alignment of these records and the extent of the EECO are not precise, because of stratigraphic issues revealed and discussed in the text. Nevertheless, there appears a major

1443 switch from morozovellids to acarininids at the species level, independent of abundance,
1444 sometime within the EECO.
1445
1446 **Figure 2.** Approximate locations for the three sites discussed in this work. Also shown is Site
1447 1258, which has a bulk carbonate $\delta^{13}C$ record spanning the EECO. Base map is from
1448 http://www.odsn/de/services/paleomap.html.
1449
1450 **Figure 3**. The Possagno section in northeast Italy when sampled in the Carcoselle quarry
1451 between Summer 2002 and Spring 2003 (Photo by Luca Giusberti, Summer 2002).
1452 Lower panel shows the then exposed quarry face. Upper panel shows the geological map
1453 comprising the Mesozoic–Cenozoic pelagic formations (modified from Braga, 1970). 1.
1454 Quaternary deposits; 2, 3. Calcarenite di Castelcucco (Miocene); 4. Glauconitic arenites
1455 (Miocene); 5. Siltstones and conglomerates (upper Oligocene-lower Miocene); 6. Upper
1456 Marna di Possagno (upper Eocene); 7. Formazione di Pradelgiglio (upper Eocene); 8. Marna
1457 di Possagno (upper Eocene); 9. Scaglia Cinerea (middle-upper Eocene); 10. Scaglia Rossa
1458 (upper Cretaceous-lower Eocene); 11. Faults; 12. Traces of the stratigraphic sections
1459 originally studied by Bolli (1975). The outcrop sampled in 2003 was located very close to the
1460 outcrops sampled in the sixties (dotted red circle).
1461
1462 **Figure 4.** Lithology, stratigraphy, and bulk sediment stable-isotope composition of the
1463 Possagno section aligned according to depth. The planktic foraminiferal biozones follow
1464 those of Wade et al. (2011), as modified by Luciani and Giusberti (2014).
1465 Magnetostratigraphy and key calcareous nannofossil events come from Agnini et al. (2006).
1466 *S. rad*.= *Sphenolithus radians*; T.c./T.o.= *Tribrachiatus contortus/ Tribrachiatus orthostylus;*
1467 *D. lod*.= *Discoaster lodoensis*; Tow.=*Toweius*; *T. orth*.= *Tribrachiatus orthostylus*; *D.*

sublod.= *Discoaster sublodoensis*. The stable isotope records come from this study (red and blue). Established early Eocene "events" are superimposed in light red; suggested carbon isotope excursions (CIEs) within the EECO are shown with numbers. 1= Limestone, 2= Marly limestones and calcareous marls, 3= cyclical marl-limestone alternations, 4= Marls, 5=Clay marly units (CMU).

Figure 5. Cores, stratigraphy, and bulk sediment stable isotope composition for the early Eocene interval at Deep-Sea Drilling Project (DSDP) Site 577 aligned according to composite depth. The Wade et al. (2011) E-zonation, partly modified by Luciani and Giusberti (2014), has been applied to Site 577 on the basis of the events recorded by Lu (1995) and Lu and Keller (1995). The base of Zone E3 has been positioned at the top of *Morozovella velascoensis,* even though this event is uncertain due to the lowest core gap. The lowest occurrence of *Morozovella formosa* occurs within C24r in agreement with Wade et al. (2011) and defines the E3/E4 zonal boundary. The base of M. *aragonensis*, defining the E4/E5 zonal boundary, is recorded within C24n, in agreement with Luciani and Giusberti (2014). The boundary between Zones E5 and E6 cannot be placed by means of the *M. subbotinae* top because this species disappears (at Site 577) much earlier with respect to the expected C23n top (Wade et al., 2011), i.e., in middle C24n, even below the base of *M. aragonensis.* Our new interpretation of the magnetostratigraphy at Site 1051, based on calcareous nannofossil events (see text), substantiates the significant diachrony of this biohorizon. We have therefore positioned, at Site 577, the upper boundary of Zone E5 at the lowest occurrence of *Acarinina aspensis,* according to the original definition of Zone E5 by Berggren and Pearson (2005). Due to the absence of *Astrorotalia palmerae* at Site 577 and to diachronous appearance of *A. cuneicametrata* base we cannot differentiate between Zone E6 and Zone E7a.

Cores are aligned following Dickens and Backman (2013), with an increased gap between Core 577*-8H and Core 577*-9H (see text). Magnetostratigraphy and key calcareous nannofossil events are those summarized by Dickens and Backman (2013). *F.* spp.= *Fasciculithus spp.*; *D. dia.= Discoaster diastypus*; T.c./T.o.= *Tribrachiatus contortus/ Tribrachiatus orthostylus; D. lod.= Discoaster lodoensis*; *T. orth.= Tribrachiatus orthostylus; D. sublod.= Discoaster sublodoensis*. The stable isotope records come from Cramer et al. (2003) – black – and this study (red and blue). Established early Eocene "events" are superimposed in light red; suggested carbon isotope excursions (CIEs) following the "L event" (yellow band) are shown with numbers.

Figure 6. The Possagno section and its $\delta^{13}C$ record (**Figure 4**) with measured relative abundances of primary planktic foraminiferal genera, fragmentation index (*F* index) and coarse fraction. The subbotinid abundance includes both *Subbotina* and *Parasubbotina* genera. Note that the EECO and several carbon isotope excursions (CIEs) before and after it are marked by a significant increase in *Acarinina* abundance. Note also the major decline in abundance of *Morozovella* at the start of the EECO. Filled yellow circles show occurrences of abundant radiolarians. Lithological symbols as in **Figure 4**.

Figure 7. The early Eocene succession at DSDP Site 577 and its $\delta^{13}C$ record (**Figure 5**) with measured relative abundances of primary planktic foraminifera genera (Lu, 1995; Lu and Keller, 1995). The Wade et al. (2011) E-zonation, partly modified by Luciani and Giusberti (2014), has been applied to Site 577 on the basis of the events recorded by Lu (1995) and Lu and Keller (1995). *F.* spp.= *Fasciculithus spp.*; *D. dia.= Discoaster diastypus*; T.c./T.o.= *Tribrachiatus contortus/ Tribrachiatus orthostylus; D. lod.= Discoaster lodoensis*; *T. orth.= Tribrachiatus orthostylus; D. sublod.= Discoaster sublodoensis*. Suggested carbon isotope

1518 excursions (CIEs) following the "L event" are shown with numbers. The subbotinid
1519 abundance includes both *Subbotina* and *Parasubbotina* genera. Note also that the major
1520 switch from *Morozovella* to *Acarinina* approximately coincides with the "J event", the top of
1521 polarity chron C24n, and the start of EECO.
1522
1523 **Figure 8.** Lithology, stratigraphy, bulk sediment $\delta^{13}C$ composition, relative abundances of
1524 primary planktic foraminiferal genera, and fragmentation index (*F* index) for the early
1525 Eocene interval at ODP Site 1051. The planktic foraminiferal biozones follow those of Wade
1526 et al. (2011), as modified by Luciani and Giusberti (2014; see **Figure 1** caption).
1527 Magnetostratigraphy and positions of key calcareous nannofossil events come from Ogg and
1528 Bardot (2001) and Mita (2001), but with an important modification to polarity chron labeling
1529 (see text and Cramer et al., 2003). *S. rad*.= *Sphenolithus radians*; *D. lod*.= *Discoaster*
1530 *lodoensis*; *Tow*.= *Toweius*; *T. orth*.= *Tribrachiatus orthostylus*; *D.sub*.= *Discoaster*
1531 *sublodoensis.* The $\delta^{13}C$ record comes from Cramer et al. (2003). Foraminferal information
1532 comes from this study, subbotinids include both *Subbotina* and *Parasubbotina*. Established
1533 early Eocene "events" are superimposed in light red.
1534
1535 **Figure 9.** Carbon isotope and paleomagnetic records across the early Eocene for the
1536 Possagno section, DSDP Site 577, and ODP Site 1258 (Kirtland-Turner et al., 2014). This
1537 highlights the overall framework of carbon cycling in the early Eocene, but also stratigraphic
1538 problems across the EECO at each of the three sites. At Possagno, the coarse resolution of
1539 isotope records and the condensed interval at C23r and upper C24n makes correlations
1540 difficult. At DSDP Site 577, the entire record is compressed in the depth domain.
1541 Nonetheless, a major shift in frequency and amplitude of CIEs appears to have happened

1542 during the EECO. Suggested carbon isotope excursions (CIEs) that probably correlate within
1543 the EECO are shown with numbers.
1544
1545 **Figure 10.** Abundance patterns of primary planktic foraminiferal taxa from the Farra section,
1546 cropping out 50 km NE of Possagno, plotted against bulk sediment $\delta^{13}C$, $CaCO_3$ content, *F*
1547 index and magnetostratigraphy. The *Subbotina* group includes besides *Subbotina,* the genera
1548 *Parasubbotina* and *Globorotaloides* that constitute the minor component of this group. All
1549 data are from Agnini et al. (2009). Note that the switch in abundance between *Morozovella*
1550 and *Acarinina* occurs close the "J event".
1551
1552 **Figure 11**. The record of warm-indices symbiont-bearing morozovellids and large
1553 acarininids (>200 micron) in the western Tethyan setting from the Possagno (below, this
1554 paper) and Alano sections (above, from Luciani et al., 2010) plotted against the generalized
1555 oxygen and carbon isotopic curves based on benthic foraminiferal record shown in
1556 Vandenberghe et al. (2012, Fig. 28.11; slightly modified). The original oxygen and carbon
1557 isotopic values from Cramer et al. (2009) are recalibrated to GTS2012 (Vandenberghe et al.,
1558 2012). The Tethyan record shows that the long-lasting EECO and MECO intervals of intense
1559 warmth mark two main steps in the decline of relative abundance within this group of
1560 important early Paleogene calcifiers, which almost completely disappeared at about 38 Ma,
1561 near the Bartonian/Priabonian boundary (Agnini et al., 2011; Luciani et al., 2010; Wade,
1562 2004; Wade et al., 2012). E-Zones follow Wade et al. (2011), partly modified by Luciani and
1563 Giusberti (2014).
1564
1565
1566

Supplementary material

Table S1. Carbon and oxygen isotopes from the Possagno section.

Table S2. Carbon and oxygen isotopes from DSDP Site 577.

Table S3. Foraminiferal abundances, fragmentation index (%) and coarse fraction (%) from the Possagno section.

Table S4. Foraminiferal abundances from DSDP Site 577.

Table S5. Foraminiferal abundances from ODP Site 1051.

Figure S1. The Possagno $\delta^{13}C$ data and relative abundance of minor planktic foraminiferal genera and selected species plotted against lithology and fragmentation index (*F* index) data. Magnetostratigraphy is from Agnini et al. (2006). The biozonal scheme is from Wade et al. (2011), modified by Luciani and Giusberti (2014). Established early Eocene "events" are superimposed in light red; suggested carbon isotope excursions (CIEs) within the EECO are shown with numbers. Lithological symbols as in figure 4.

Appendix A: Taxonomic list of planktic forainiferal species cited in text and figures

Globanomalina australiformis (Jenkins, 1965)

Morozovella aequa (Cushman and Renz, 1942)

Morozovella gracilis (Bolli, 1957)

Morozovella lensiformis (Subbotina, 1953),

Morozovella marginodentata (Subbotina, 1953)

Morozovella subbotinae (Morozova, 1939)

Parasubbotina eoclava Coxall, Huber and Pearson, 2003

Parasubbotina griffinae (Blow, 1979)

Parasubbotina pseudowilsoni Olsson and Pearson, 2006

Subbotina corpulenta (Subbotina, 1953)

Subbotina eocena (Guembel, 1868)

Subbotina hagni (Gohrbandt, 1967)

Subbotina senni (Beckmann, 1953)

Subbotina yeguanesis (Weinzierl and Applin, 1929*)*

Planoglobanomalina pseudoalgeriana Olsson & Hemleben, 2006

Appendix B: Taxonomic list of calcareous nannofossil taxa cited in text and figures

Discoaster diastypus Bramlette and Sullivan 1961

Discoaster lodoensis Bramlette and Sullivan 1961

Discoaster sublodoensis Bramlette and Sullivan 1961

Fasciculithus Bramlette and Sullivan 1961

Fasciculithus tympaniformis Hay and Mohler in Hay et al. 1967

Sphenolithus radians Defandre in Grassé 1952

Toweius Hay and Mohler 1967

Tribrachiatus contortus (Stradner 1958) Bukry 1972

*Tribrachiatus orthostylus (*Bramlette and Riedel 1954) Shamrai 1963

Figure 1

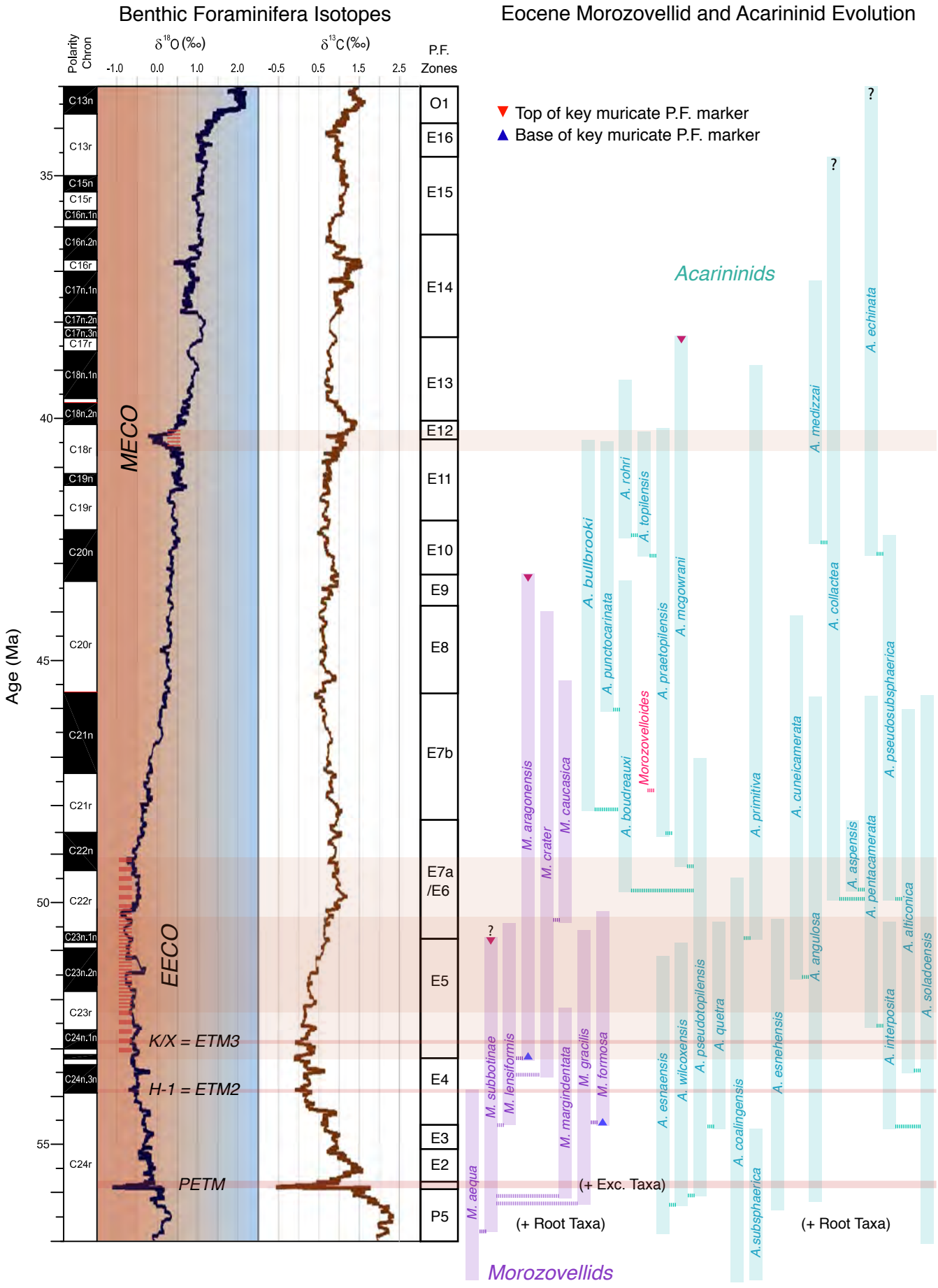
Benthic Foraminifera Isotopes
Eocene Morozovellid and Acarininid Evolution
Polarity Chron
δ18O (‰)
δ13C (‰)
P.F. Zones
Age (Ma)
MECO
EECO
K/X = ETM3
H-1 = ETM2
PETM
Top of key muricate P.F. marker
Base of key muricate P.F. marker
Acarininids
Morozovellids
(+ Root Taxa)
(+ Exc. Taxa)
(+ Root Taxa)
M. aragonensis
M. crater
M. caucasica
M. subbotinae
M. lensiformis
M. marginodentata
M. gracilis
M. formosa
M. aequa
A. bullbrooki
A. punctocarinata
A. boudreauxi
A. rohri
A. topilensis
Morozovelloides
A. praetopilensis
A. medizzai
A. collactea
A. echinata
A. aspensis
A. pentacamerata
A. pseudosubsphaerica
A. alticonica
A. soladoensis
A. interposita
A. cuneicamerata
A. angulosa
A. esnehensis
A. primitiva
A. esnaensis
A. wilcoxensis
A. pseudotopilensis
A. quetra
A. coalingensis
A.subsphaerica

Figure 2

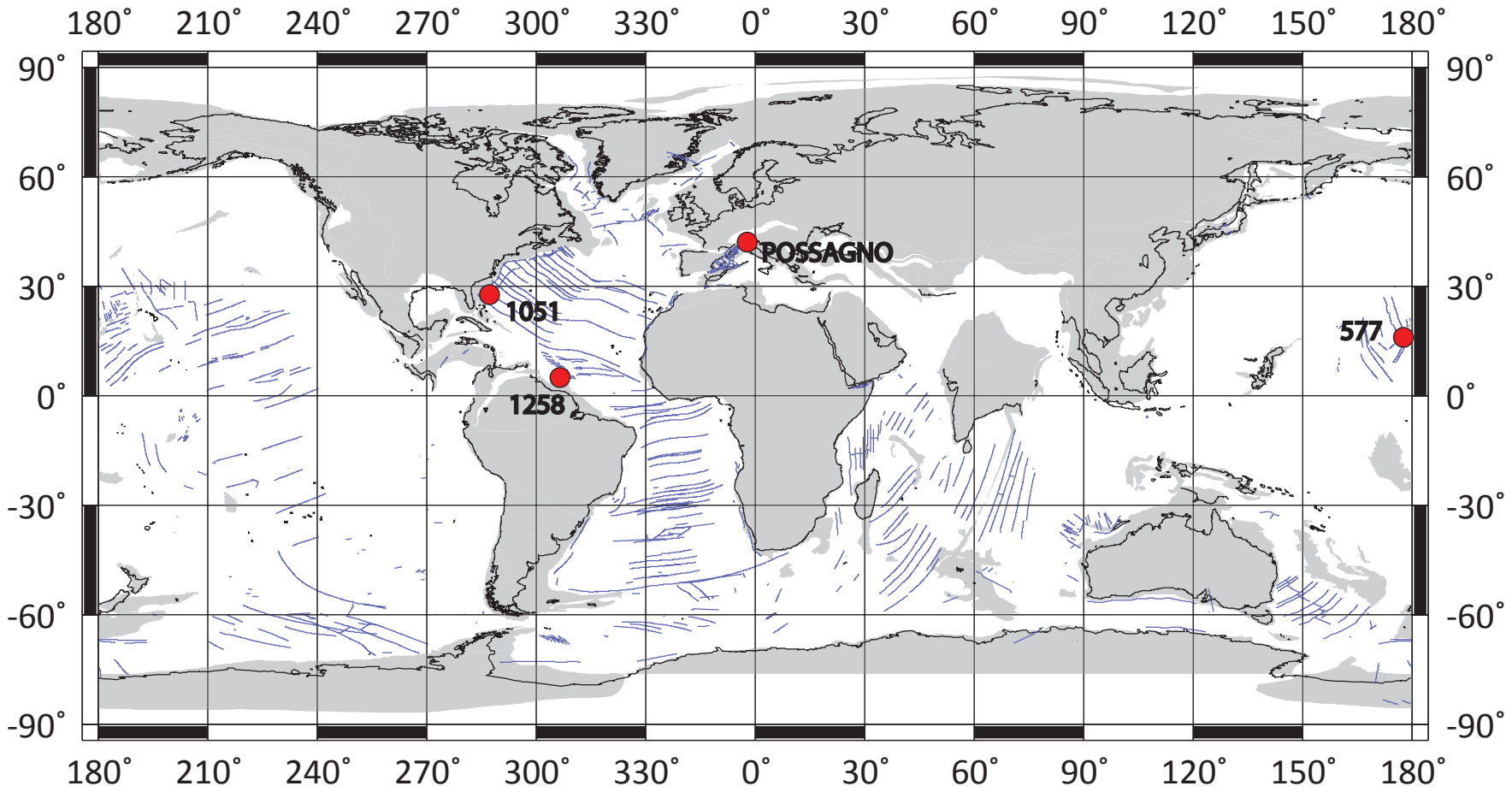

50 Ma Reconstruction

Figure 3

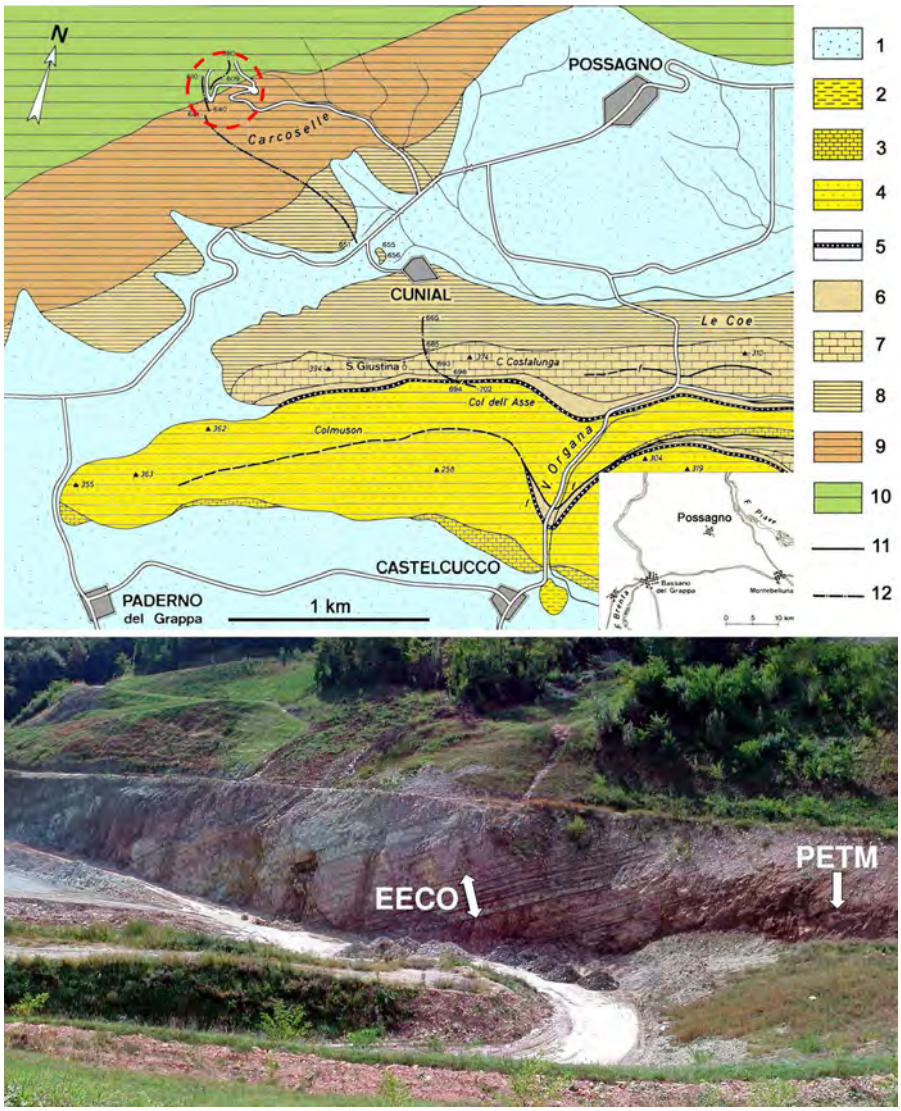
N
POSSAGNO
Carcoselle
CUNIAL
Le Coe
C Costalunga
S. Giustina
Col dell' Asse
Colmuson
V. Organa
CASTELCUCCO
PADERNO
del Grappa
1 km
Possagno
1
2
3
4
5
6
7
8
9
10
11
12
EECO
PETM

Figure 4

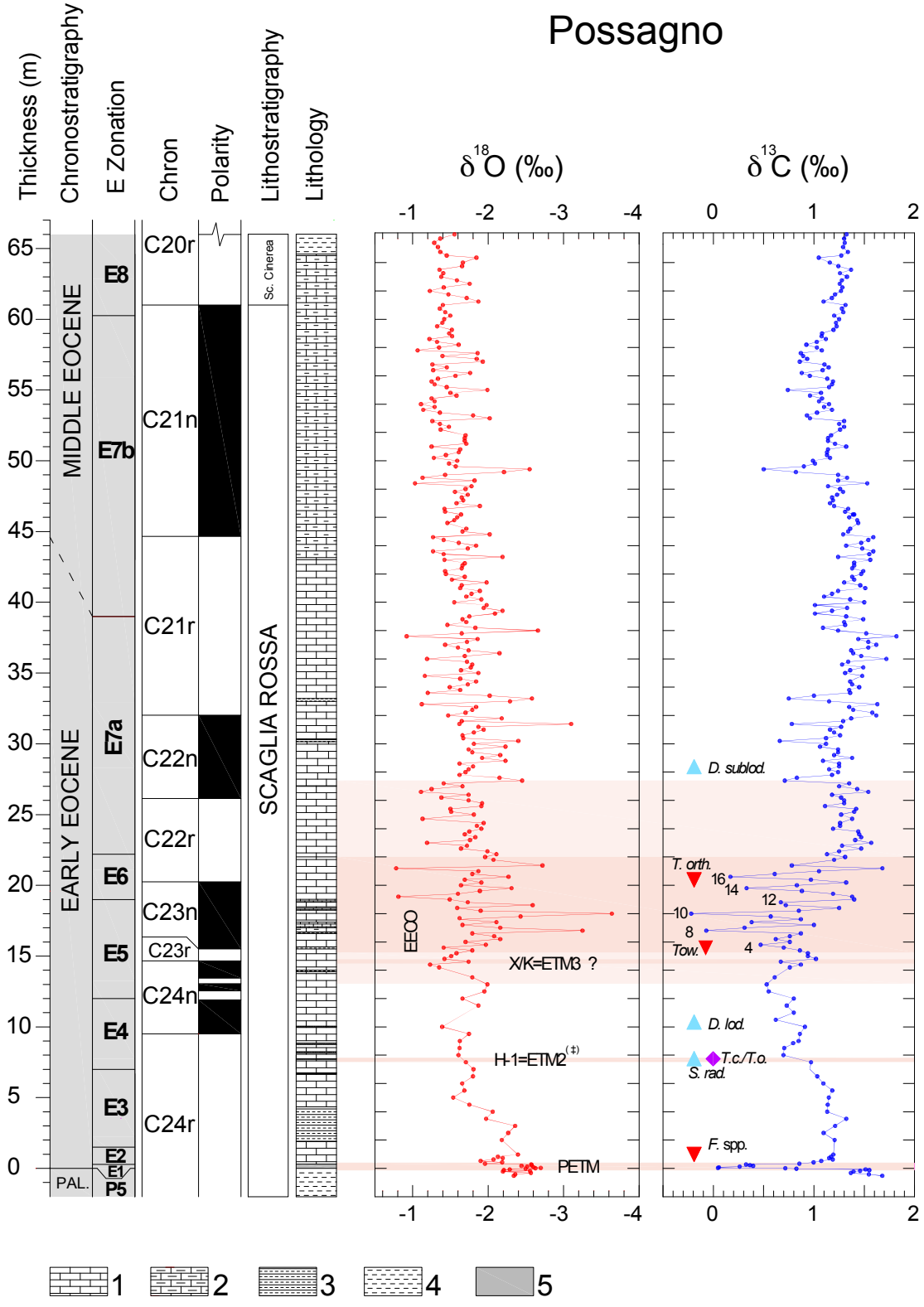
Possagno
Thickness (m)
Chronostratigraphy
E Zonation
Chron
Polarity
Lithostratigraphy
Lithology
δ18O (‰)
δ13C (‰)
MIDDLE EOCENE
EARLY EOCENE
PAL.
E8
E7b
E7a
E6
E5
E4
E3
E2
E1
P5
C20r
C21n
C21r
C22n
C22r
C23n
C23r
C24n
C24r
Sc. Cinerea
SCAGLIA ROSSA
EECO
X/K=ETM3 ?
H-1=ETM2(‡)
PETM
D. sublod.
T. orth.
Tow.
D. lod.
T.c./T.o.
S. rad.
F. spp.
1
2
3
4
5

Figure 5

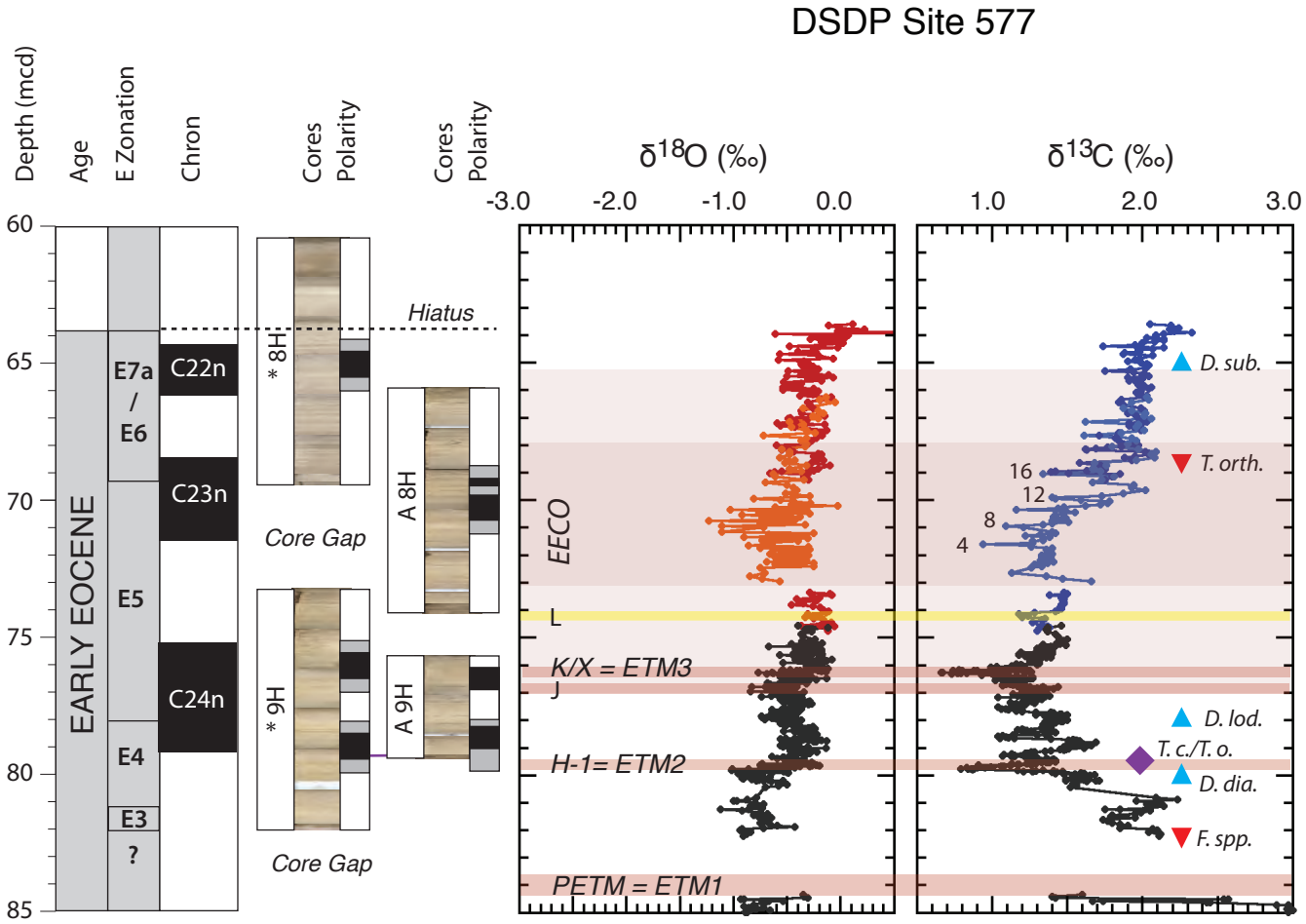
DSDP Site 577
Depth (mcd)
Age
E Zonation
Chron
Cores Polarity
Cores Polarity
δ18O (‰)
δ13C (‰)
-3.0
-2.0
-1.0
0.0
1.0
2.0
3.0
60
65
70
75
80
85
EARLY EOCENE
E7a / E6
E5
E4
E3
?
C22n
C23n
C24n
* 8H
* 9H
A 8H
A 9H
Hiatus
Core Gap
Core Gap
EECO
L
K/X = ETM3
J
H-1= ETM2
PETM = ETM1
16
12
8
4
D. sub.
T. orth.
D. lod.
T. c./T. o.
D. dia.
F. spp.

Figure 6

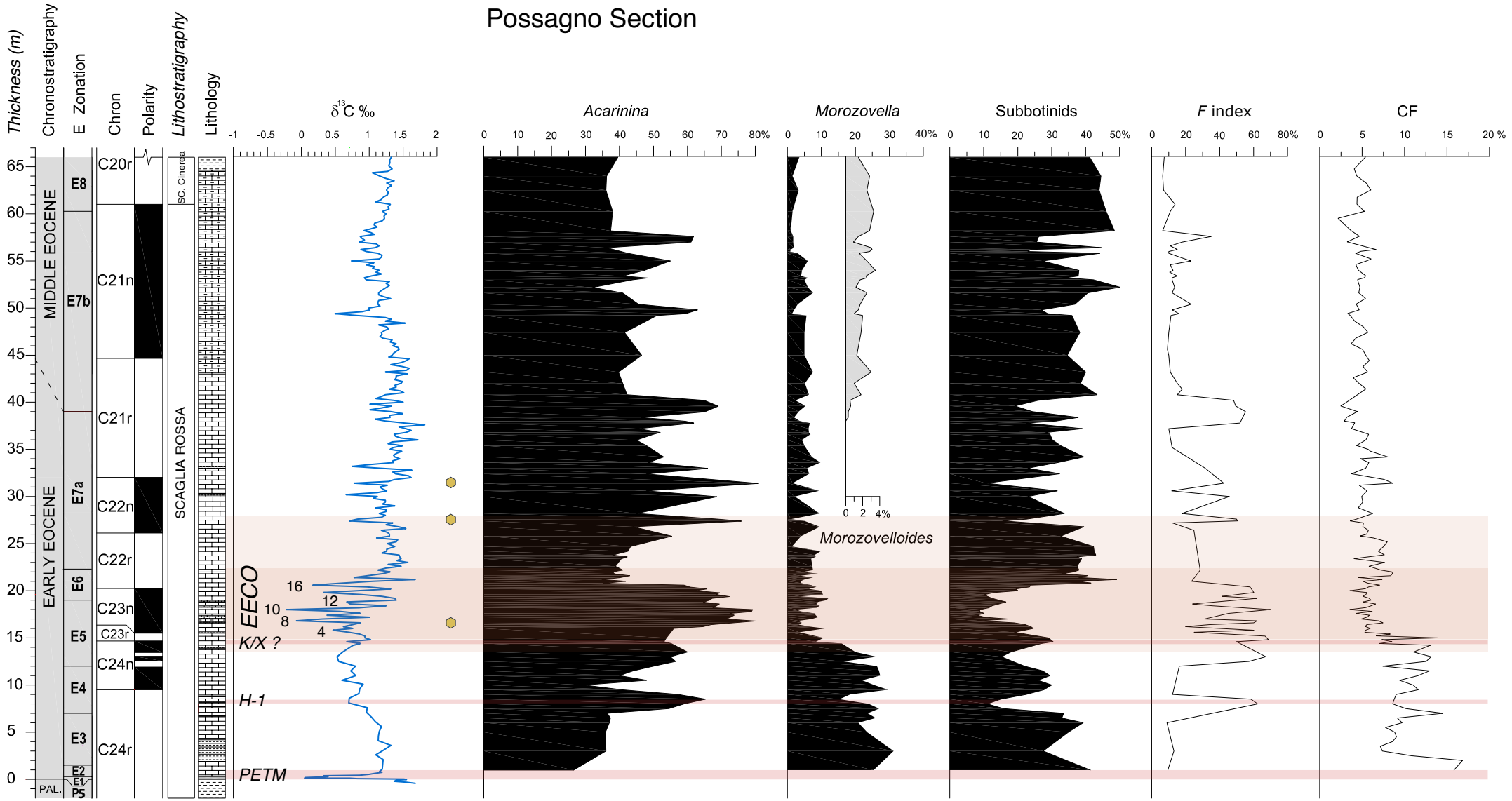
Possagno Section
Thickness (m)
Chronostratigraphy
E Zonation
Chron
Polarity
Lithostratigraphy
Lithology
δ13C ‰
Acarinina
Morozovella
Morozovelloides
Subbotinids
F index
CF
MIDDLE EOCENE
EARLY EOCENE
PAL.
E8
E7b
E7a
E6
E5
E4
E3
E2
E1
P5
C20r
C21n
C21r
C22n
C22r
C23n
C23r
C24n
C24r
SC. Cinerea
SCAGLIA ROSSA
EECO
K/X ?
H-1
PETM

Figure 7

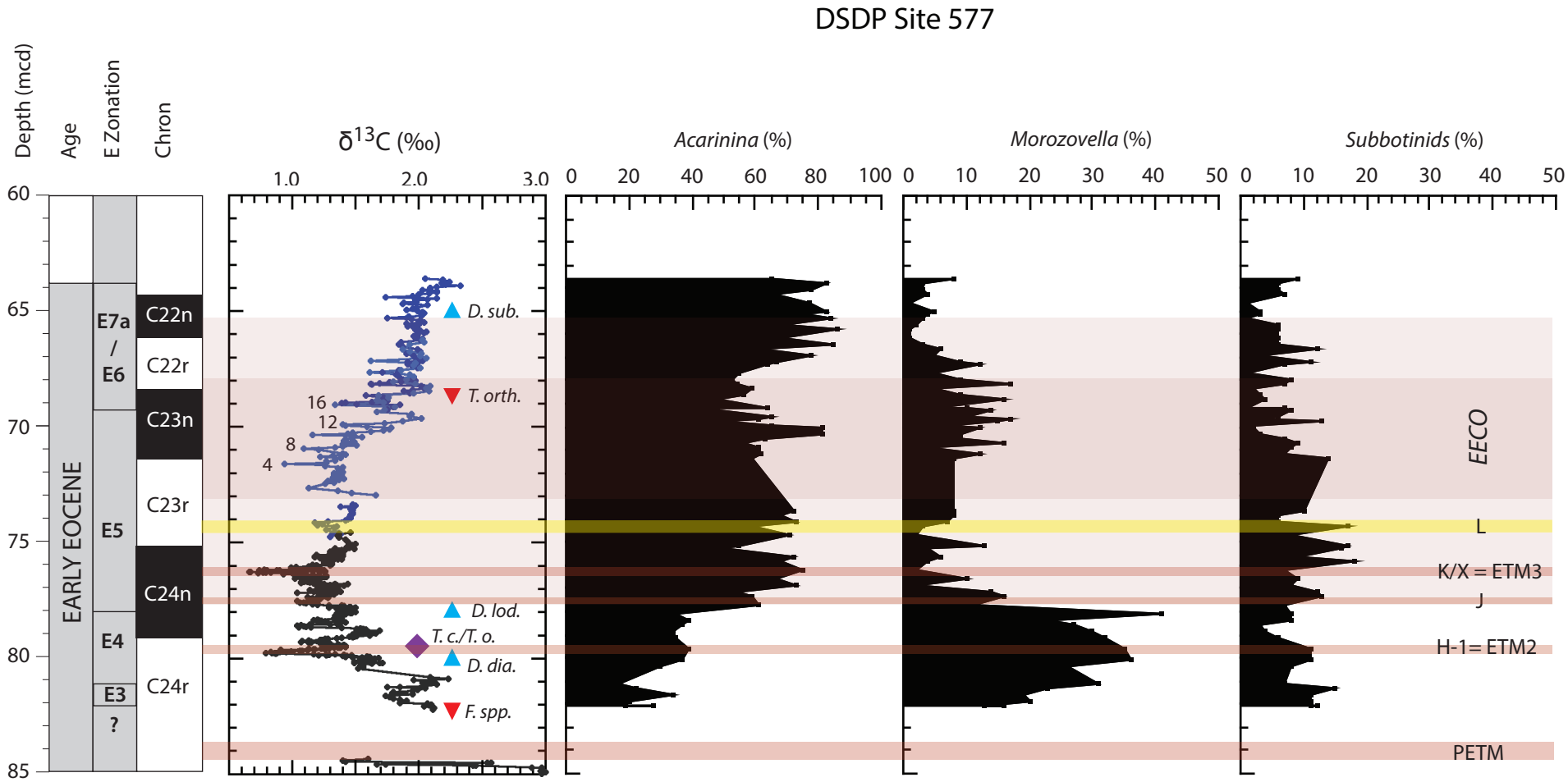
DSDP Site 577
Depth (mcd)
Age
E Zonation
Chron
EARLY EOCENE
E7a / E6
E5
E4
E3
?
C22n
C22r
C23n
C23r
C24n
C24r
60
65
70
75
80
85
δ13C (‰)
1.0
2.0
3.0
16
12
8
4
D. sub.
T. orth.
D. lod.
T. c./T. o.
D. dia.
F. spp.
Acarinina (%)
0
20
40
60
80
100
Morozovella (%)
0
10
20
30
40
50
Subbotinids (%)
0
10
20
30
40
50
EECO
L
K/X = ETM3
J
H-1= ETM2
PETM

Figure 8

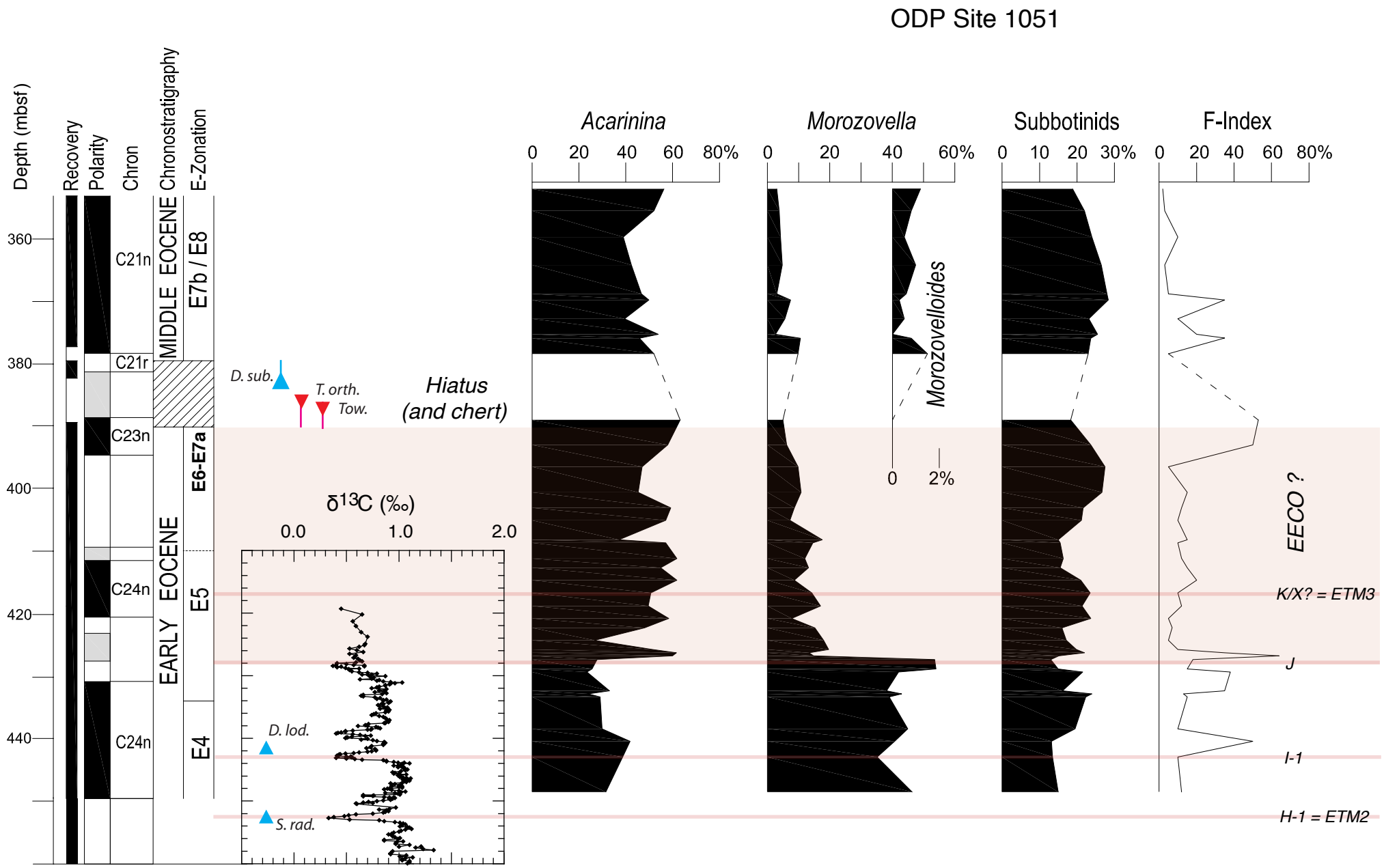
ODP Site 1051
Depth (mbsf)
Recovery
Polarity
Chron
Chronostratigraphy
E-Zonation
360
380
400
420
440
C21n
C21r
C23n
C24n
C24n
MIDDLE EOCENE
EARLY EOCENE
E7b / E8
E6-E7a
E5
E4
D. sub.
T. orth.
Tow.
Hiatus
(and chert)
δ13C (‰)
0.0
1.0
2.0
D. lod.
S. rad.
Acarinina
0
20
40
60
80%
Morozovella
0
20
40
60%
Morozovelloides
0
2%
Subbotinids
0
10
20
30%
F-Index
0
20
40
60
80%
EECO ?
K/X? = ETM3
J
I-1
H-1 = ETM2

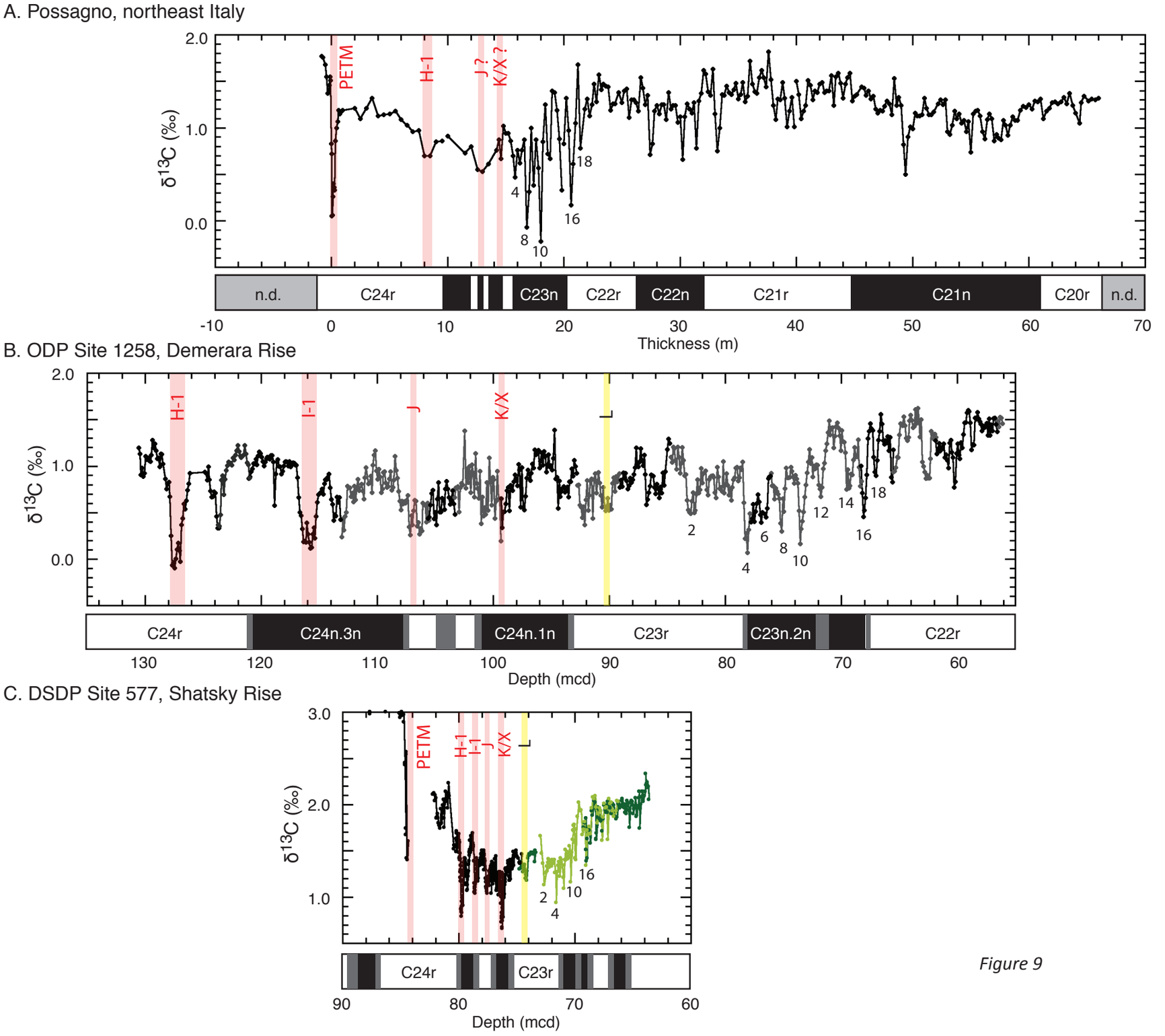
A. Possagno, northeast Italy
PETM
H-1
J ?
K/X ?
δ13C (‰)
2.0
1.0
0.0
4
8
10
16
18
n.d.
C24r
C23n
C22r
C22n
C21r
C21n
C20r
n.d.
-10
0
10
20
30
40
50
60
70
Thickness (m)
B. ODP Site 1258, Demerara Rise
H-1
I-1
J
K/X
δ13C (‰)
2.0
1.0
0.0
2
4
6
8
10
12
14
16
18
C24r
C24n.3n
C24n.1n
C23r
C23n.2n
C22r
130
120
110
100
90
80
70
60
Depth (mcd)
C. DSDP Site 577, Shatsky Rise
PETM
H-1
I-1
J
K/X
δ13C (‰)
3.0
2.0
1.0
2
4
10
16
C24r
C23r
90
80
70
60
Depth (mcd)

Figure 9

Figure 10

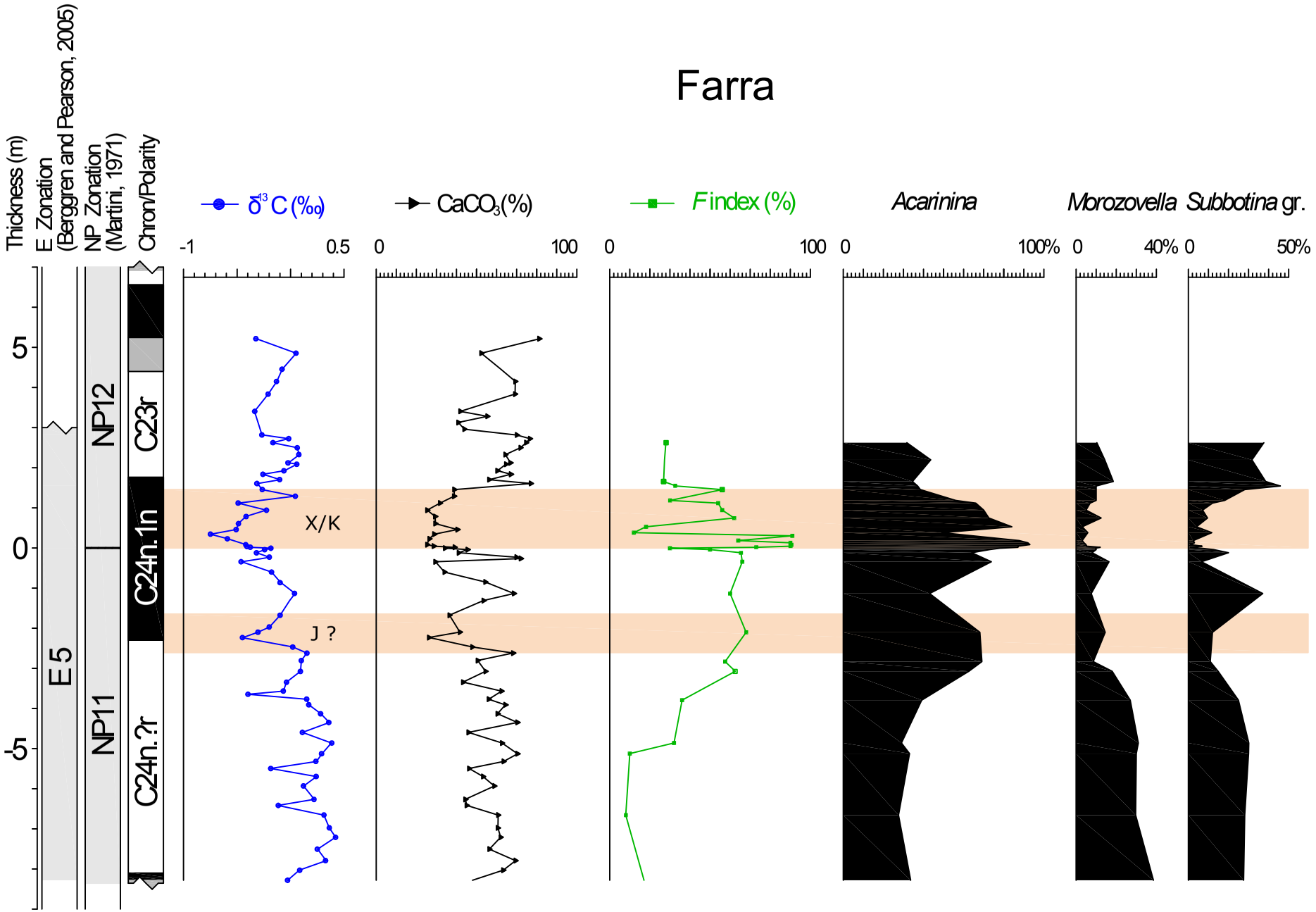
Farra
Thickness (m)
E Zonation (Berggren and Pearson, 2005)
NP Zonation (Martini, 1971)
Chron/Polarity
δ13C (‰)
CaCO3(%)
Findex (%)
Acarinina
Morozovella
Subbotina gr.
-1
0.5
0
100
0
100
0
100%
0
40%
0
50%
5
0
-5
E 5
NP12
NP11
C23r
C24n.1n
C24n.?r
X/K
J ?

Figure 11

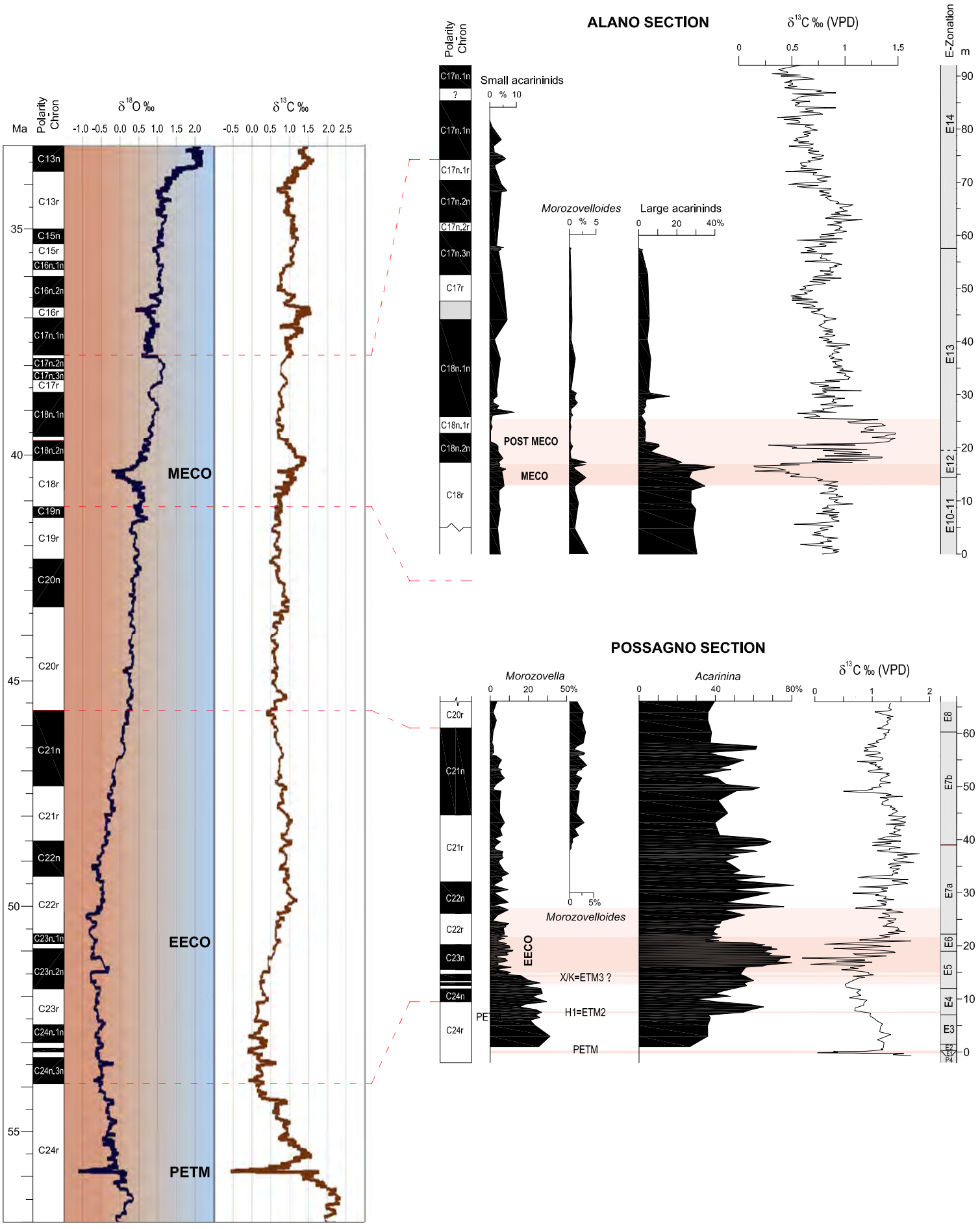
ALANO SECTION
POSSAGNO SECTION
Ma
Polarity Chron
δ18O ‰
δ13C ‰
δ13C ‰ (VPD)
E-Zonation
m
Small acarininids
Morozovelloides
Large acarininds
POST MECO
MECO
Morozovella
Acarinina
EECO
X/K=ETM3 ?
H1=ETM2
PETM
PE
C13n
C13r
C15n
C15r
C16n.1n
C16n.2n
C16r
C17n.1n
C17n.2n
C17n.3n
C17r
C18n.1n
C18n.2n
C18r
C19n
C19r
C20n
C20r
C21n
C21r
C22n
C22r
C23n.1n
C23n.2n
C23r
C24n.1n
C24n.3n
C24r
C17n.1r
C17n.2r
C18n.1r
C18n.2r
E14
E13
E12
E10-11
E8
E7b
E7a
E6
E5
E4
E3
E2
P4